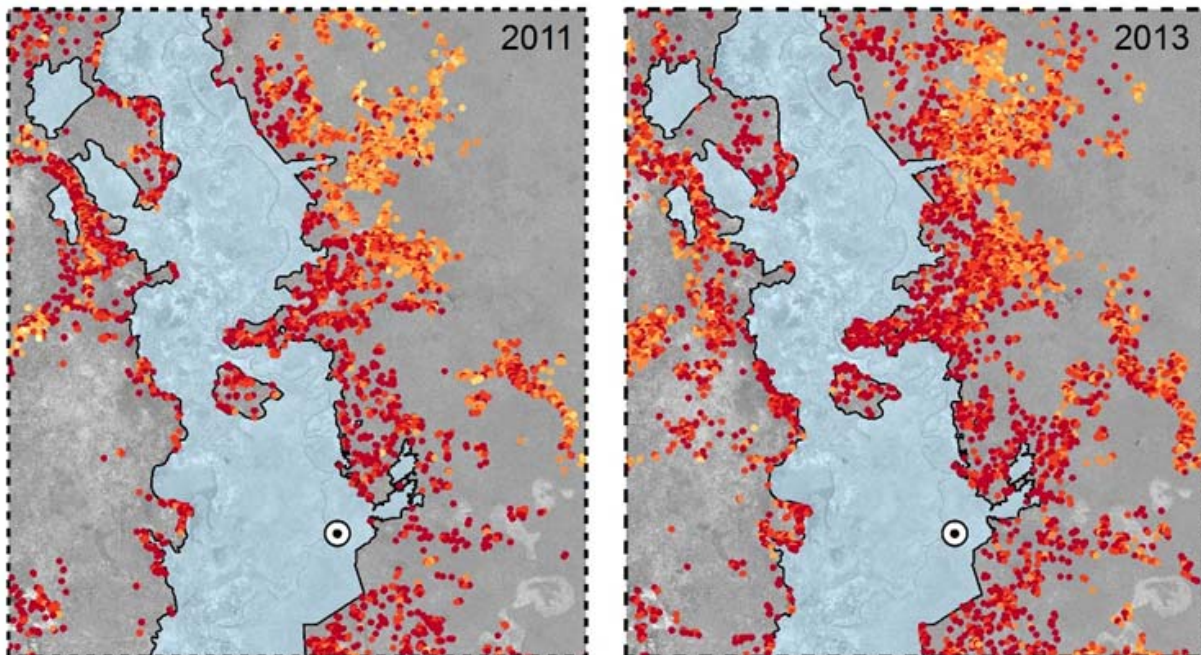


Detection of Charcoal Production Sites on Southern Somalia Using Very High Resolution Imagery



Project Report

March 2014



Somalia Water and Land Information Management
Ngecha Road, Lake View. P.O Box 30470-00100, Nairobi, Kenya.
Tel +254 020 4000300 - Fax +254 020 4000333,
Email: swalim@fao.org Website: <http://www.faoswalim.org>



The designations employed and the presentation of material in this information product do not imply the expression of any opinion whatsoever on the part of the Food and Agriculture Organization of the United Nations and the SWALIM Project concerning the legal status of any country, territory, city or area of its authorities, or concerning the delimitation of its frontiers or boundaries.

This document should be cited as follows:

^{1,2}Bolognesi M., ¹Leonardi U., ²Vrieling A., ³Rembold F., ¹Gadain H. 2014. Detection of Charcoal Production Sites in Southern Somalia Using Very High Resolution Imagery. Technical Project Report. FAO-SWALIM, Nairobi, Kenya.

¹ FAO-SWALIM, Nairobi, Kenya.

² ITC, Faculty of Geo-Information Science and Earth Observation of the University of Twente, Enschede, the Netherlands.

³ EC-JRC, Ispra, Italy.

ABSTRACT

Following more than 20 years of civil unrest, environmental information for Southern Somalia is scarce while there is clear evidence that the war economy fuelled by the conflict is rapidly depleting the country's natural resources, especially the woody biomass. Wood charcoal production is one of the most relevant businesses supporting war regimes such as the extreme Islamist group Al Shabaab, which has ruled in Southern Somalia from 2006 to 2012 and is still occupying large areas. In this study, we first used Very High Resolution (VHR) satellite imagery of early 2011 and early 2013 for developing a semi-automatic mapping method of charcoal production sites as a proxy of tree loss over a 6000 km² area along the Juba River in Southern Somalia. The user's accuracy of semi-automatic charcoal production site detection varied between 81.7% for 2011 and 87.3% for 2013, while the producer's accuracy was 68.2% and 65.5% respectively and, as compared to visual interpretation, reduced significantly the required time. The analysis of the changes between the two dates led to an average tree loss estimation of 3.3%, corresponding to 520,520 trees over the 2 years period. The results help to better understand the dimension and impact of charcoal production in Southern Somalia and are a first step towards the development of a charcoal production monitoring system.

ACKNOWLEDGEMENTS

The authors wish to acknowledge the considerable support given by the U.S. Department of State (USDS) for providing very high resolution satellite imagery (WorldView-1) for this study.

We also wish to acknowledge the contributions from our colleagues at FAO-SWALIM in different areas.

Copyright

Image property U.S. Department of State.

WorldView-1 © DigitalGlobe.

Provided to FAO-Somalia under NextView License.

TABLE OF CONTENTS

1.	INTRODUCTION.....	7
2.	STUDY AREA AND DATA	9
2.1.	STUDY AREA.....	9
2.2.	DATA.....	12
3.	METHODS.....	14
3.1.	CHARCOAL SITE DETECTION	14
3.2.	CHANGE DETECTION	19
3.3.	WOOD VOLUME AND TREE LOSS ESTIMATION.....	20
4.	RESULTS	23
4.1.	CHARCOAL SITE DETECTION	23
4.2.	CHANGE DETECTION	27
4.3.	WOOD VOLUME AND TREE LOSS ESTIMATION.....	33
5.	DISCUSSION.....	35
6.	CONCLUSIONS	38

LIST OF FIGURES

Figure 1 – Study Area. Large contiguous areas of agricultural land were digitized by visual interpretation and excluded from the research analysis as charcoal production only occur where natural vegetation is found.....	10
Figure 2 - War in Somalia: Map of Al Shabaab Control	11
Figure 3 – Available images and coverage. 2011 coverage on the left, and 2013 on the right. All images were acquired during the main dry season.....	12
Figure 4 – Difference in Sun and satellites elevation and azimuth angles. An example of angle differences between 2011 dates.	13
Figure 5 - Object Bases Image Analysis workflow. Once segments are created, a progressive selection is executed based on specified thresholds. While the Threshold-based rules produce a selection of the segments as outputs, the Merge and Watershed processes create new segments requiring new selection, which is obtained by applying new Threshold rules (reflectance and size rules). The final output consists of the objects target of the analysis, charcoal production sites.....	15
Figure 6 - One-dimensional example of watershed algorithm commonly used to separate segments. Local maxima define watershed lines, which split the segments.	16
Figure 7 - Example of dark objects classified as charcoal sites. The one indicated by the arrow has reflectance, shape, and size within the thresholds, but in fact corresponds to a tree casting a shadow. The subset is part of the 1x1 km pilot area, used for the development of the rule set (19 February 2013 scene).	17
Figure 8 – Two-stage sampling strategy. 1) First stage: creation of 1x1 km grids and random selection; 2) Second stage: visual identification of sites contained in each randomly selected grid; 3) Charcoal sites appear on images as dark dots and are visually identifiable.....	18
Figure 9 – Timber mound before being buried. Screen shot from a Puntland Development Research Center (PDRC) video.....	20
Figure 10 – Visual interpretation of a 1x1 km cluster with semi-automatically detected sites, but no visual counts. It reveals that erroneously detected sites are due to shadows, caused by a land cover type composed by dark and tall vegetation.....	24
Figure 11 – Example of semi-automatically detected charcoal sites grouped by radius size.	24
Figure 12 – Subset of the study area showing clearly visible charcoal production sites in 2011 (left) that are becoming less visible in 2013 (right), i.e. several years after charcoal is produced in the site.....	27
Figure 13 – Appearance of kiln covered by soil (A, C), and with remaining charcoal ashes exposed (B, D). A and C are from an 18 February 2011 scene, while B and D from 3 March 2011.....	28
Figure 14 (left) – Spatial distribution of charcoal production detected with the object-based classification using 2011 and 2013 WorldView-1 imagery. Charcoal sites are grouped by 1x1 km grid cells, and coloured in yellow/red tonalities according to the number of sites per grid. Darker red correspond to grids containing a higher number of detected sites.	30
Figure 15 (right) – Map showing changes in the detected number of sites per grid (1x1 km) between 2011 and 2013.....	30
Figure 16 – Overview of main charcoal production areas that were semi-automatically detected, and visually-delineated road network. Straight lines are main dirt roads running through the bush land, while curved lines can be seen mostly in relation to charcoal production areas.....	31
Figure 17 - Routes running close to charcoal sites do not follow straight lines. Example of the road network expansion between 2011 and 2013, with the purpose to access trees and produce charcoal. Note	

how new roads leads to new charcoal sites (black dots), following an opportunistic plan to get closer to trees.....	32
Figure 18 - Satellite record of the same area, showing shadow casting difference due to differences in elevation and sun angles of satellite and Sun. Angles are more similar in the image on the left, and	35

LIST OF TABLES

Table 1 - Image metadata: Elevation and Azimuth angles of the available images.	13
Table 2 - Accuracy assessment results.....	23
Table 3 – Classification results by site size.....	25
Table 4 – Producer's accuracy	26
Table 5 – Detected sites grouped by size. Number of sites detected on 2011 scenes, and number of sites for 2013 not previously detected on 2011 scenes. To be noted the overall increase in the number of sites.	29
Table 6 – From kiln size to quantification of dry wood used, and charcoal and charcoal bags produced. Reported values are averages. To determine the mean and standard deviation I used all combinations of assumed low/high values for dry wood used, charcoal production, and charcoal bags produced, calculated for each site radius.....	34

1. INTRODUCTION

In developing countries wood fuels account for between 50 and 90 percent of the energy used (FAO, 2010). The wood fuel related market is an important source of income for a significant number of people (Clancy, 2008). Despite the fact that empirical evidence is lacking to support wood fuel collection as a key driver of deforestation on a global scale (Cooke et al., 2008), evidence exists that at the local level it can have significant impacts on forest degradation (FAO, 2010; Kanninen et al., 2007). Wood fuel refers to any energy source that comes from woody biomass. These cover a range of fuels, including fuelwood, charcoal, industrial fuelwood, wood pellets, biogas, cellulosic ethanol, and other forms of bioenergy. Charcoal is a wood fuel made from burning wood in a low-oxygen environment, and produces more heat and energy per kilogram than wood (UCS, 2011). According to FAO statistics, Africa produces 55 per cent of the global charcoal production (FAO, 2010). However, these charcoal production estimates are often inaccurate when disaggregated at the national level. For many African countries, detailed information is lacking, and estimates are consequently based on analytical and projection models that use wood fuel information of countries in similar socioeconomic and geographical situations, or by multiplying the country population by a per capita estimate based on a literature review carried out in 1980 (Whiteman et al., 2002; Wardle and Pontecorvo, 1981).

In Sub-Saharan Africa wood fuel is the main source of household energy (Zulu & Richardson, 2013). Especially in urban areas, it is mainly used in the form of charcoal, as it is easier to transport and burns more efficiently than fuel wood (Akpalu et al., 2011). Studies conducted in West Africa suggest that levels of wood fuel harvesting are generally balanced with the productive capacity of the wood stocks, and that accelerated rates of deforestation occur when the intensity of wood fuel production prevent regeneration and therefore sustainable production (Ribot, 1998).

In Somalia, wood fuel production is not only triggered by domestic consumption, but also by foreign demand. In fact, charcoal has developed into one of the major export products, and is sometimes referred to as “black gold” (Bakonyi & Abdullani, 2006; UN Security Council, 2011). UNEP (2005) estimated that 4.4 million trees are logged annually to produce the 250 thousand tonnes of charcoal that are exported every year from Somalia to Saudi Arabia, Yemen and the United Arab Emirates. According to FAO estimates the charcoal production grew from about 180 thousand tonnes in 1961 to almost 1.2 million tonnes in 2012, with a much steeper increase after 1991, when the estimated production was nearly 420 thousand (FAO, 2013). Since the collapse of Somalia’s central government in 1991, militia groups are fighting for political control, and finance their activities partly with illegal charcoal exports (UN Security Council, 2011). For this reasons, in February 2012 the UN Security Council has banned charcoal export from Somalia. The charcoal trade is suggested to be the main driver of the fast depletion experienced by forests and woodlands of Somalia (UNEP, 2005).

Despite the known high exports of charcoal from Somalia, and the potential contribution to tree cover loss, little quantitative information on tree cover loss in Somalia during the past two decades is available. Reduction of vegetation cover, loss of topsoil, and gully erosion have been identified as the main types of land degradation in Somalia (Omuto et al., 2009). Trees help to control soil erosion and protect cropland and pasture (Richardson, 2010). By destroying the protective tree cover, tree cutting for charcoal production contributes to land degradation, together with overgrazing, continuous mono-cropping, and inefficient irrigation (Omuto et al., 2009). Somalia is predicted to be one of the nine African countries that will face

water scarcity by 2025 (Boko et al., 2007), and deforestation and associated land degradation will worsen the water scarcity effects by increasing the population's vulnerability to drought (Holleman, 2003). Existing studies on tree cover loss have focused on the north-eastern part of Somalia (MPDES-CHE, 2004; Oduori et al., 2009), because here the better security situation permitted the execution of fieldwork. For example, a recent study investigated tree loss of an area located in the arid Soole-Sanag Plateau, in Northern Somalia, characterised by sparse vegetation (Oduori et al., 2011). The researchers recorded a tree loss of 12.98% between 2001 and 2006, based on individual tree identification obtained through visual photo-interpretation of 8 sampling frames, for a total of 128 km². Another recent study, estimated a tree loss of 7.2% over the period 2006-2012 for two sample areas covering about 60 km² in southern Somalia (Rembold et al., 2013). Given the limited security in large parts of Somalia in the last 20 years, and especially in the Southern and Central parts of country since 2006 when the Islamist group called Al Shabaab took control, direct evidence of tree cover changes can almost exclusively be obtained through remote sensing. Using medium resolution MODIS imagery (500m), Miles et al. (2006) assessed the distribution of tropical dry-forest at the global scale. However, for charcoal production in Somalia, tree cover clearances typically occur at a small-scale and in a patchy distribution (Oduori et al., 2011) that may not be detected, or at least not accurately, following change detection with MODIS-type imagery (Ryan et al. 2002). DeFries et al. (2007) suggest that for monitoring small-scale changes in forest cover the use of aerial photos or high resolution (10-60m) satellite imagery is more appropriate. Studies in northern Somalia indicate that accurate estimation of tree-cutting rates requires the detection of changes in the presence of individual trees (Oduori et al., 2009; Oroda et al., 2007). Rembold et al. (2013) suggest that for areas where individual trees are difficult to detect, loss of tree cover can be estimated by the identification of charcoal production sites, multiplied by the estimated average amount of trees burnt at each site. For detecting single objects from remotely sensed data, the spatial resolution should be less than half the object size (Woodcock & Strahler, 1987). For detecting individual trees or alternatively small charcoal production sites in Somalia, therefore, only aerial photos and very high resolution (<5m) imagery provide the required resolution.

Studying land cover changes using sub-meter satellite imagery is financially demanding, given the high image cost per square kilometre, and the costs for image interpretation. It is also technically challenging when similar spectral characteristics of different vegetation types do not allow a clear visual discrimination of trees from dense shrubland, as is the case of the Acacia – Commiphora deciduous bushland and thicket ecoregion, which covers the greater part of Somalia (White, 1983). The identification of charcoal production sites could then be a good alternative, because they form clear round objects, and are spectrally different from the surroundings (Rembold et al., 2013). An important question is whether charcoal production sites can be identified in a rapid way for large areas from very high resolution (VHR) imagery, hence reducing interpretation costs. The objectives of this study are:

- To develop a semi-automated method to accurately map and quantify charcoal production sites in the study area in southern Somalia from very high resolution satellite imagery;
- To identify and explain changes in the number and location of charcoal production sites over the period 2011-2013;
- To estimate volume of timber used for charcoal production and related tree loss.

The outcomes can be used to infer evidence of areas where charcoal activity is taking place. Such evidence will highlight zones potentially affected by land degradation, in addition to providing indication on Al-Shabaab controlled areas in the region.

2. STUDY AREA AND DATA

2.1. Study area

I refined the study area boundaries by considering the area covered by 2013 imagery that was also available for 2011 (about 6,000 km²). The final area of interest used for this research comprised a strip of land of about 4,700 km², extending along the Juba River for an extent about 50 km wide and 115 km long, and lying between the city of Bu'aale in the north and the port city of Kismayo in the south (Figure 1). According to the general classification of Africa's vegetation by White (1983) the study area consists of Acacia-Commiphora deciduous bushland and thicket, a primarily semi-arid savannah with thorn bushes. Species of these two genera dominate the vegetation throughout most of the region, with exceptions consisting of small stands of Terminalia species. A detailed description of the vegetation within the study area does not exist, and there is no field data confirming distribution and density of tree species. An inventory conducted by Bird and Sheperd (1989) described the vegetation type for a neighbouring area extending from Saako, about 80 km north of the northern limit of my study area, to Awdiinle (200km north-east of Saako). Evergreen members of the Caparidaceae are frequently grazed and thus are repeatedly prevented from growing above the bush layer (Bird and Shepherd, 1989).

There are four distinct seasons: two rainy seasons (Gu – April to June, and Dayr – October to November), and two dry seasons (Jiilaal, the main one – December to March, and Xagga – July to September). The mean annual rainfall ranges between 500 and 750 mm. The Juba river floodplain, included in the study area, is one of the most fertile lands of Somalia (SWALIM, 2010).

The communities living in the area of study are mainly agro-pastoralists depending on livestock and maize for their livelihood. Most of the agriculture is irrigated with one of the following three systems: small-scale pump-fed surface irrigation of cash crops; small-scale gravity-fed surface irrigation of staple and cash crops; spate and flood recession irrigation of staple crops (FAO, 2005). During the cultivation period (Gu and Deyr rains) animals are moved away from the farming areas (FSNAU, 2014). Livestock depends entirely on the natural vegetation, while agricultural crops are grown on a small scale and are used mainly for home consumption. Pastoralists have to rely on trees and shrubs as the only fodder source for their livestock, especially during the dry season when the grass cover disappears (Runge, 1998).

The charcoal production method carried on in the study area is known as the Bay Method, and it was described by Robinson (1988). To produce charcoal, a type of oven known as 'kiln' is used. Kilns are built by piling the timber straight on the soil floor. The timber is collected from the surroundings and arranged into a circular mound designed, with stronger poles erected at the centre, and other shorter pieces of wood positioned around it. The mound is packed as close as possible, and the gaps are filled with smaller pieces of wood, shrubs, and grass to facilitate kiln lighting. The whole structure is then buried with sand and iron sheets. Once the burning process is completed, the charcoal is formed and it is loaded into bags, leaving a layer of black ashes on the ground. This dark ring of ashes is visible on very high resolution imagery, such as WorldView-1. Somali experts confirm that kilns are used in a single event and mostly during dry seasons. A study conducted on the Bay Method (Robinson, 1988) revealed a carbonization time ranging from 3 to 8 days, and a cooling time ranging between 9 and 12 days, depending on timber's quality, quantity, and moisture content. The same research (Robinson, 1988) indicates that the timber necessary to build a kiln is traditionally collected by donkey and cart and taken to a central site, near the site where the timber has been felled, and the furthest distance covered in the case of evaluation trials was 200 m.

From the imagery available (see Section 2.2), I digitized large contiguous areas of agricultural land by visual interpretation (based on neat field lines, fences, roads, and villages). These areas can be easily and quickly

identified, and I excluded them from the research analysis, since charcoal production only occur where natural vegetation is found.

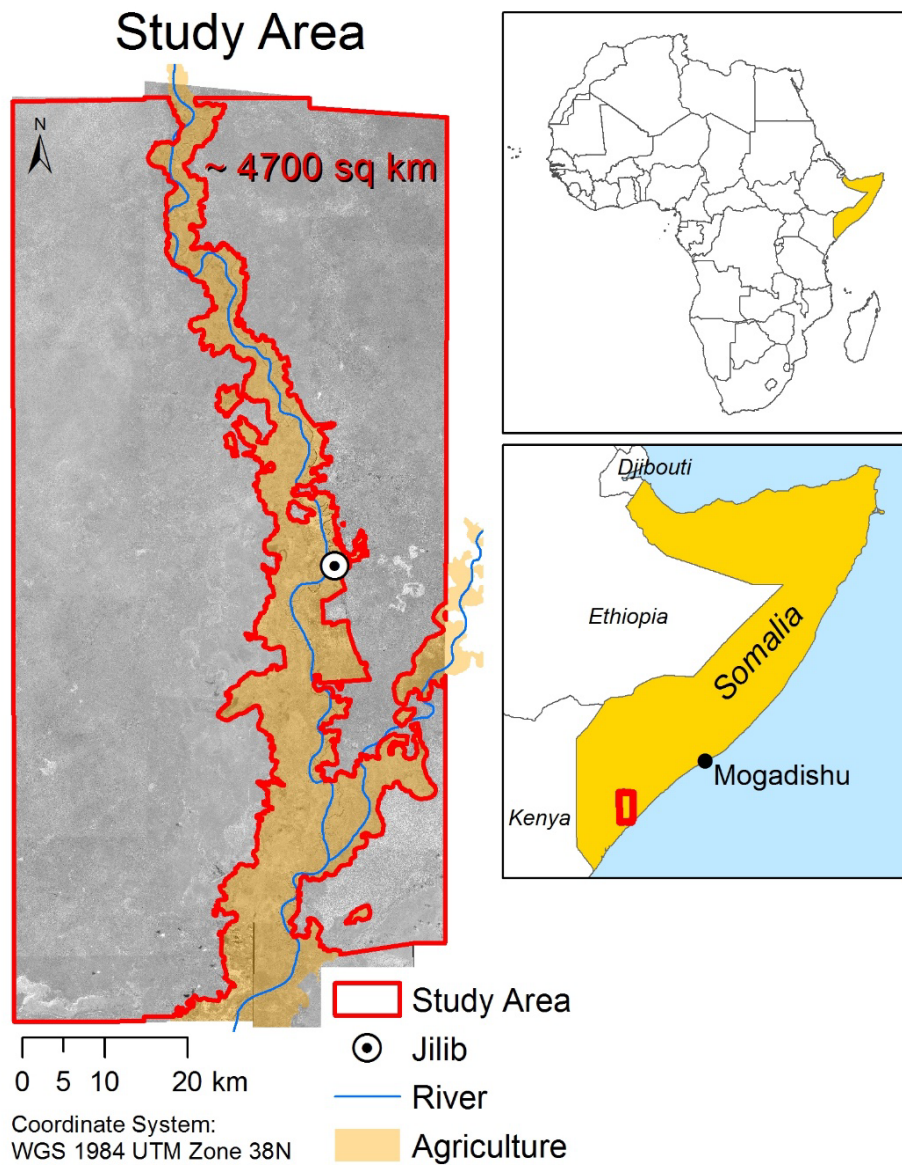


Figure 1 – Study Area. Large contiguous areas of agricultural land were digitized by visual interpretation and excluded from the research analysis as charcoal production only occur where natural vegetation is found.

The socio-political context of the area is very unstable and hard to delineate (Figure 2). After the capture of Kismayo port by Kenyan forces in September 2012, conflicts over political power arose. Local groups declared an autonomous area called Jubaland, which claimed three of the surrounding administrative regions (Gedo, Lower Juba and Middle Juba) as a federal state of Somalia. At first, the central government in Mogadishu opposed to Jubaland's formation, and political conflict and confusion continued. Finally, on 28 August 2013 Jubaland Administration signed an agreement with the Somalia Federal Government (Garoweonline, 2014a). However, on 12 September 2013 the leader of Somalia's Jubaland survived an attack carried out by Al Shabaab terrorist group, highlighting the instability of the political situation of the area (Garoweonline, 2014b).

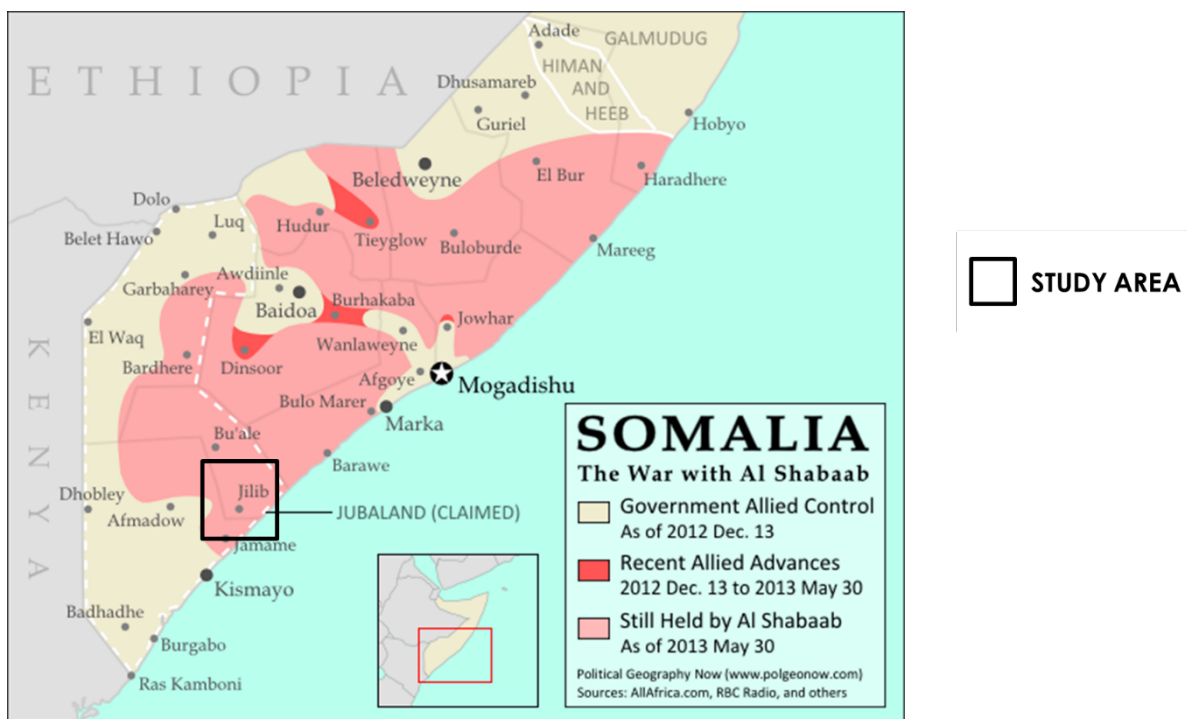


Figure 2 - War in Somalia: Map of Al Shabaab Control.
(Source: <http://www.polgeonow.com/2013/05/somalia-war-map-al-shabaab-2013.html>)

2.2. Data

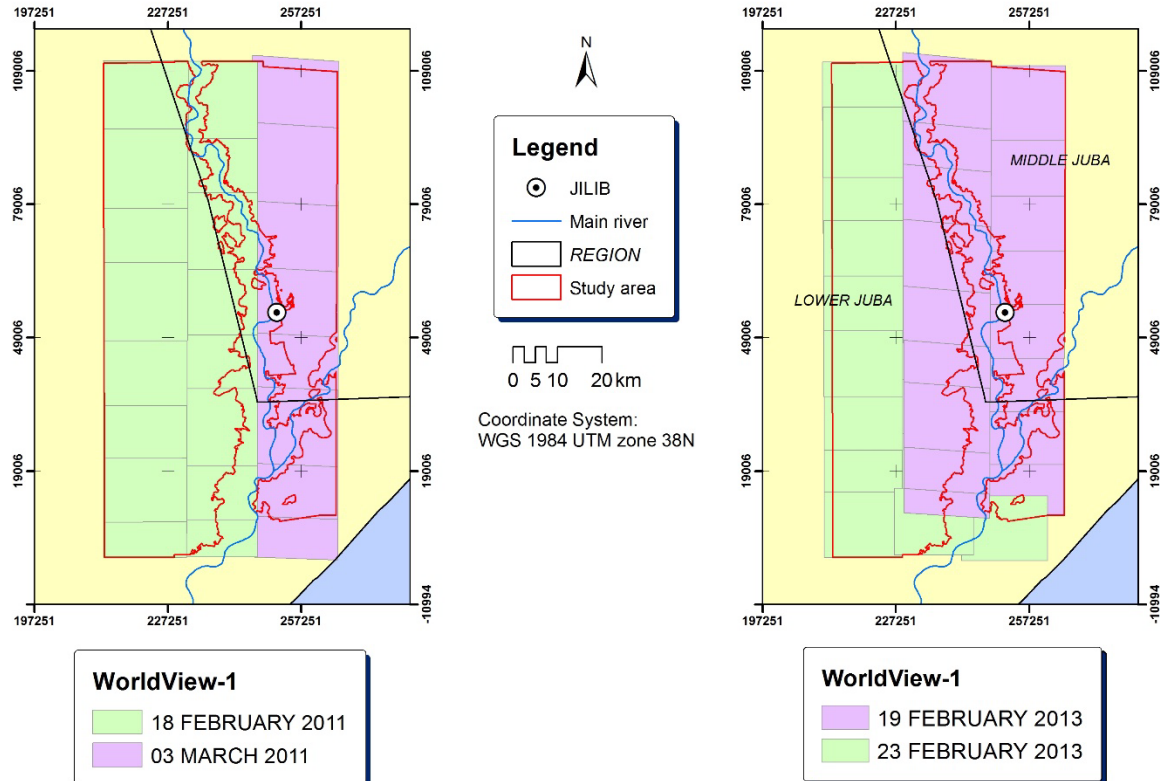


Figure 3 – Available images and coverage. 2011 coverage on the left, and 2013 on the right. All images were acquired during the main dry season.

WorldView-1 imagery was available for an area of nearly 6,000 km² in the south-western part of Somalia (Figure 3) for February and March 2011 (16 scenes of 18 February and 8 scenes of 3 March) and for February 2013 (16 scenes of 19 February and 11 scenes of 23 February). All images were acquired during the main dry season (Jiilaal) of the respective year. The satellites therefore recorded the land cover in similar climatic conditions.

The WorldView-1 sensor produces panchromatic images with a resolution of 0.5 m. The archive was provided by the US Department of State to FAO Somalia under the NextView License. Images were provided in National Imagery Transformation format (NTIF) which contains the image band compressed in a Jpeg2000 format and all the image metadata in an internal XML-like file. All scenes were received spatially referenced to the World Geodetic System – 1984 (GCS_WGS_1984).

The raw Digital Number (DN) values were transformed into Top-of-Atmosphere (TOA) reflectance values using the conversion parameters delivered with every WorldView-1 product and located in the image metadata files (IMD), and following the equations described by the image provider (Digital Globe, 2010). The metadata files also report the elevation and azimuth angles of both Sun and satellites at the time of image acquisition (Table 1). The elevation angle is the angle between the horizon and the line of sight, measured in the vertical plane, while the azimuth angle is measured from true north clockwise on the horizontal plane (Figure 4).

Table 1 - Image metadata: Elevation and Azimuth angles of the available images.

	18 Feb 2011	03 Mar 2011	19 Feb 2013	23 Feb 2013
<i>Sun Elevation</i>	65.0	66.2	61.0	63.0
<i>Sat Elevation</i>	87.4	69.2	63.3	72.1
<i>Sun Azimuth</i>	120.3	109.5	115.7	112.4
<i>Sat Azimuth</i>	127.8	129.4	151.0	188.1

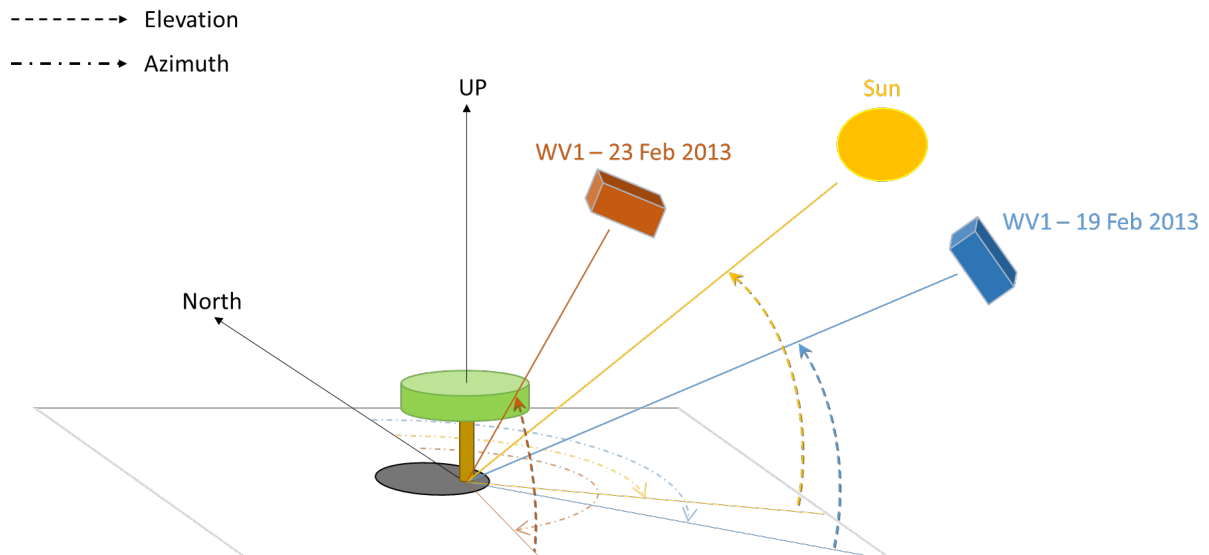


Figure 4 – Difference in Sun and satellites elevation and azimuth angles. An example of angle differences between 2013 dates.

3. METHODS

3.1. CHARCOAL SITE DETECTION

3.1.1. OBJECT BASED IMAGE ANALYSIS

While in Rembold et al. (2013) charcoal production site detection was based on visual image interpretation, the present study focusses on the development of an object-based image analysis (OBIA) approach for a rapid identification of charcoal production areas.

OBIA attempts to translate the human visual perception into rules to identify image objects in semi-automatic ways, increasing the repeatability and production, while reducing time and costs (Hay & Castilla, 2006). The basis of OBIA is the grouping of pixels into segments, then classified into meaningful objects based on their spatial and spectral homogeneity. The segmentation is a bottom-up region merging technique. It begins considering each pixel as a separate segment, which is consequently aggregated into larger segments. The aggregation is based on homogeneity conditions set by the user, and it stops when the heterogeneity between two segments exceeds defined thresholds (Xiaoxia et al., 2005).

In this study, the software eCognition (Baatz & Schaepe, 2000; eCognition, 2013) was used to perform object-based image analysis, and the numerous segmentation options embedded were explored. In eCognition various segmentation algorithm are implemented: here we used the multi-resolution algorithm. It is an optimization procedure, which minimizes the average heterogeneity between segments and maximizes their respective homogeneity. This segmentation algorithm is based on the following key parameters:

- Scale, a unit-less parameter used to control the heterogeneity of objects, with a lower scale parameter resulting in smaller objects;
- Shape and compactness, values that modify the relationship between spectral and spatial homogeneity in order to segment data into similar regions, and that can be balanced depending on the desired output.

After setting the values for these parameters, a fully automatic step produces so called segments. By aggregating pixels into segments, statistics regarding their key parameters are retained, while additional information such as texture, geometry, and contextual information, can be used to analyse the data (eCognition, 2013). The settings of segmentation parameters depend on the data type, study area, and the objects of interest. Segment optimization aims to minimize under- and over-segmentation in order to increase the efficiency and accuracy of segments creation. Image pre-processing, for example image smoothening by a low pass filter, may assist in creating more homogenous segments, thus avoiding the creation of many small-sized ones (over-segmentation).

Various studies have developed techniques to avoid subjectivity in setting segmentation parameters. For instance, Espindola et al. (2006) proposed an objective function that uses inherent properties of remote sensing data (spatial autocorrelation and variance) to support the selection of segmentation parameters. Similarly, Draguț et al. (2010) developed a tool for an objective Estimation of Scale Parameters (ESP): it calculates the local variance of objects at different scale levels, and it indicates the scale levels at which the image can be segmented in the most appropriate manner. In this study, the ESP tool was used as it has been indicated useful when the target objects exhibit a single operational scale (Stumpf & Kerle, 2011), which is the case of charcoal production sites.

3.1.2. CHARCOAL SITE DETECTION WITH OBJECT BASED IMAGE ANALYSIS

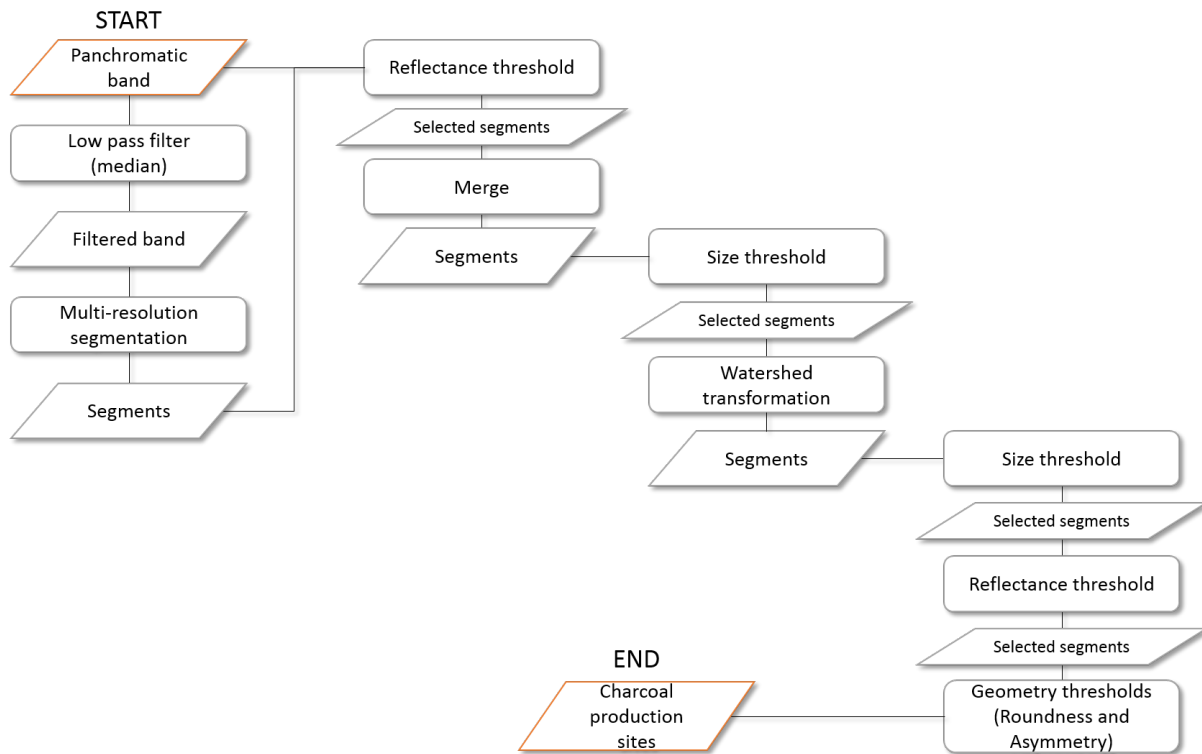


Figure 5 - Object Based Image Analysis workflow. Once segments are created, a progressive selection is executed based on specified thresholds. While the Threshold-based rules produce a selection of the segments as outputs, the Merge and Watershed processes create new segments requiring new selection, which is obtained by applying new Threshold rules (reflectance and size rules). The final output consists of the objects target of the analysis, charcoal production sites.

After applying the ESP tool to the available images and visually comparing the results, the value 37 was chosen as scale parameter: it occurred to be a common peak (highest rate of variance change) and small enough to create segments properly depicting charcoal production sites.

Charcoal production sites do not present high variability in spectral values and size, but because the heterogeneity of the images may change due to sensor characteristics and time of acquisition, unique optimal scale, shape, and compactness values valid for all images may not be expected. To develop the rule set for detecting charcoal sites (Figure 5), a 1x1 km area with a high concentration of charcoal sites was selected as pilot study area on a 19 February 2013 WorldView-1 scene. Charcoal sites within the pilot area were used as training to create an optimal rule set, and they were also counted through visual interpretation for accuracy assessment.

Prior the object based image analysis, a low-pass median filter 7x7 was applied. The filter replaces the pixel value with the median value of neighbouring pixels, therefore removing small spatial variations. After applying the median low pass filter, charcoal production sites appear as more homogeneous dark spots, reducing the internal spectral variability produced by small patchy deposits of sand or other materials, and smoothening the margins.

The eCognition multi-resolution segmentation was then applied to the filtered images. The shape and compactness parameters of the multi-resolution segmentation were selected on a trial/error basis until the segments were well delineating charcoal production sites boundaries. This was achieved setting the value of shape at 0.5 and compactness at 0.8.

Rules were subsequently constructed to identify and separate charcoal production sites from other land cover types. The parameters used were spectral reflectance, size, asymmetry, and roundness. The rule set

was built to progressively eliminate unwanted image objects (other land cover types), while keeping the identified features of interest (charcoal production sites). After the initial segmentation of filtered images, the created segments were used on the original unfiltered images to maximize the information content of each segment.

Typically, charcoal production sites appear as isolated dark spots. The first segment selection step was thus aimed at the identification of dark objects, by setting an upper threshold based on the reflectance value. The charcoal sites have a specific size of a few meters, while other dark objects that can be present within the scene (like cloud shadows or other areas burned by wildfire), tend to cover much larger surface portions. Visual interpretation revealed that charcoal production sites have a radius not exceeding 9 m, and are almost never directly adjacent to each other. For this reason, a rule was introduced to merge neighbouring segments with similar reflectance values, followed by a rule to remove large segments exceeding 254.5 m^2 (equivalent to a circle with 9 m radius), in order to retain only smaller dark segments not exceeding the size threshold. A watershed transformation (value set to 4) was applied to segments with an area lower than 254.5 m^2 to separate those charcoal production sites, which in very few cases may have also been merged because adjacent. Watershed transformation is an algorithm commonly used to separate segments. It interprets the images as height maps that are formed by basins (local minima) and ridges (local maxima). It floods the basins starting from the lowest intensity value, and creates an edge (splitting segments) where basins separated during the flood join (Figure 6).

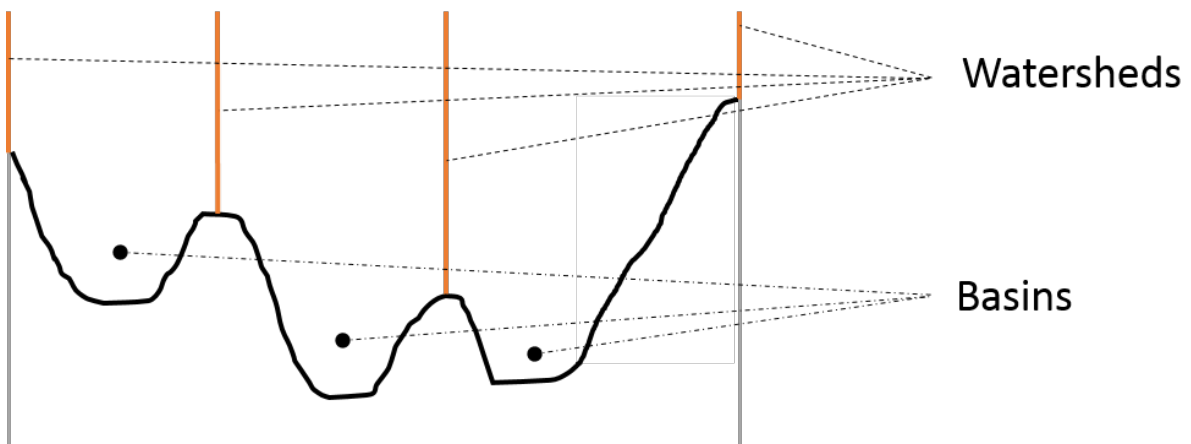


Figure 6 - One-dimensional example of watershed algorithm commonly used to separate segments. Local maxima define watershed lines, which split the segments.

Visual interpretation highlights that small-sized charcoal production sites are not always easily discernible from other dark image elements, such as tree shadows or burned agricultural residues. For this reason, an additional size-based selection was implemented within the rule set to discard all segments smaller than 28.3 m^2 (corresponding to a circle with a radius of 3 m). Although further reduced to segments within a specific range of sizes, visual inspection of the remaining selection resulted as still too broad at this stage, because of the new segments created by the merging and watershed processes. An additional selection rule was thus introduced with the definition of a precise reflectance value interval, to remove segments with a reflectance value falling outside the previously determined threshold.

Finally, rules considering the round shape typical of charcoal production sites were introduced. For each retained segment, the roundness and asymmetry parameters were calculated with eCognition. The roundness parameter expresses how similar a segment is to an ellipse, with zero as ideal value. The asymmetry parameter, instead, is the ratio of the lengths of the segment's minor and the major axes, with a low ratio indicating less differences between the axes and hence a closer similarity to a circle. The description of the rules was taken from the eCognition Developer 8.9 reference book (eCognition, 2013).

The roundness and asymmetry rules (with thresholds set at 0.45 and 0.4 respectively) enabled to remove noise caused by confusion between shadows and charcoal production sites, which have similar reflectance, but different shapes. Even during visual comparison, for small dark objects it is sometimes difficult to discriminate between charcoal production sites and tree shadows (Figure 7). The first generally tend to be rounder and larger than the second (depending on acquisition geometry of the images).

The radius size of sites was derived from the area of each segment. The implemented rule set is considering as charcoal sites only objects with an approximately round shape, and therefore their area can be considered as the one of a circle. For example, charcoal sites objects with a surface of 113.1 m² correspond to circle of 6 m radius, and with 153.9 m² to 7 m.

Following the development of the rule set for the 1x1 km pilot area, the analysis was expanded to analyse all available scenes from 19 February 2013, and then tested on the images available for the other dates. The different elevation and azimuth angles (Table 1), together with different dates of image acquisition and relative atmospheric conditions, have an influence on the reflectance values of the images. Therefore, the reflectance threshold values of the rule set were adjusted for each date, while they were kept identical among images with the same date, as unchanged were kept also all other rule settings.

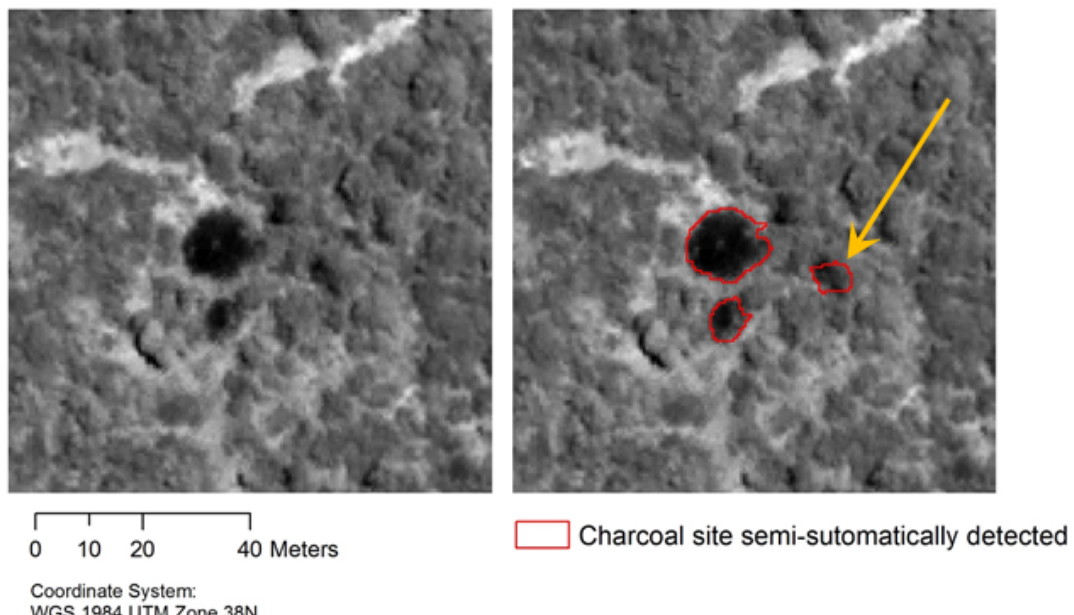


Figure 7 - Example of dark objects classified as charcoal sites. The one indicated by the arrow has reflectance, shape, and size within the thresholds, but in fact corresponds to a tree casting a shadow. The subset is part of the 1x1 km pilot area, used for the development of the rule set (19 February 2013 scene).

3.1.3. ACCURACY ASSESSMENT

A two-stage cluster sampling was implemented by building a grid of 1x1 km, to validate the capability of the developed rule set in accurately detecting the charcoal production sites across the entire satellite image coverage. A two-stage sampling is considered appropriate for studies where access to individual sample locations is particularly difficult (Köhl et al., 2006). In the first stage, a random sample of clusters was selected to cover 10% of the total natural vegetation area. In the second stage, all charcoal production sites within the selected clusters were identified by visual interpretation (Figure 8), as field work for ground truthing was not feasible due to security reasons. 419 clusters were selected and they remained the same for the analysis of both dates. The advantage of the two-stage cluster sampling for this study is the reduction of the visual interpretation to just a small random part of the entire coverage, which provides sufficient statistical support to represent the whole population, and it is used for validation purpose.

To verify the accuracy of the developed method, user's and producer's accuracy were calculated. The user's accuracy refers to the probability that a location labelled as a charcoal production site by the rule set is an actual charcoal production site (as identified from visual interpretation). The producer's accuracy refers to the probability that an actual charcoal production site is classified as such by the object based image analysis. Finally, a buffer of 200 m was created around the semi-automatically detected charcoal production sites in accordance to Robinson (1988) study (see Section 2.1). The visual interpretation of the buffer is meant to visually verify if further charcoal production sites were present in the vicinity of the semi-automatically detected sites, thus confirming that the semi-automatic analysis can offer a good indication of dominant production areas.

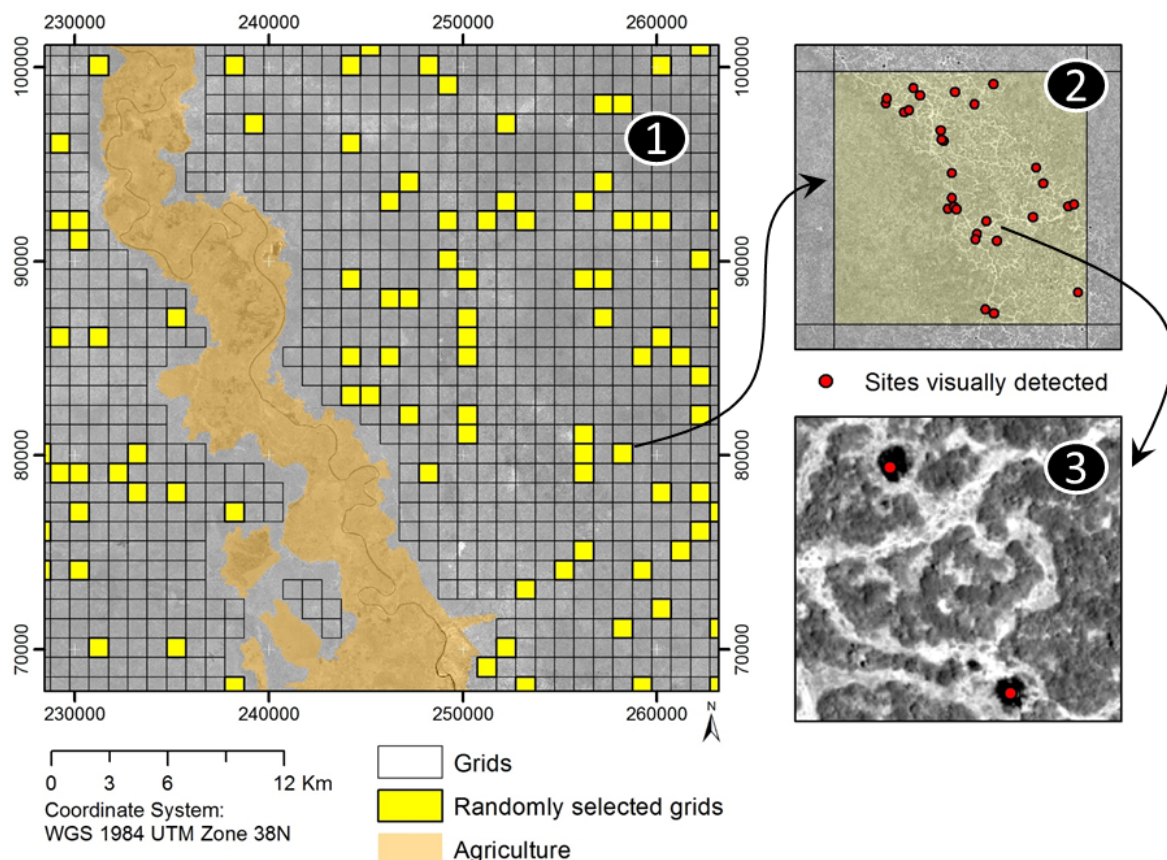


Figure 8 – Two-stage sampling strategy. 1) First stage: creation of 1x1 km grids and random selection; 2) Second stage: visual identification of sites contained in each randomly selected grid; 3) Charcoal sites appear on images as dark dots and are visually identifiable.

3.2. CHANGE DETECTION

Following the semi-automated detection of charcoal sites for 2011 and 2013 images (Section 3.1), numbers and locations of detected production sites were compared between both years. WorldView-1 products have a positional accuracy of less than 5m (Digital Globe, 2013), which is smaller than the diameter size range of charcoal production sites considered for this study (6 to 18 meters). The positional accuracy was confirmed by visual analysis of the images. This made co-registration of the images not necessary. To assess changes in locations, the 2011 and 2013 production sites were compared and results can be divided in three classes:

- Sites detected both in 2011 and 2013: since kilns are used only once (see Section 2.1), charcoal sites visible on the most recent date are just remains of sites built previously than the earlier date.
- Sites detected only in 2011: these sites were built prior the 2011 image acquisition dates. Through time they have been covered by re-growing vegetation or by soil material transported by wind, and consequently are not detectable on 2013 images. Visual inspection confirms that these sites are sometimes completely vanished. However, in some cases small dark traces can be interpreted as remains of charcoal sites, while they are not detectable by the developed semi-automated rule set, because of higher reflectance values or small size and irregular shape.
- Sites detected only in 2013: these sites were built prior the 2013 image acquisition dates, but later than 2011 scenes dates. They give a spatial indication on recent charcoal production zones.

To better understand the development of charcoal production site locations, the road network of the study area was completely digitized for both years. During digitization, both main roads and secondary paths were considered. The main purpose was to examine the spatial relationship between road presence and charcoal production sites, and to evaluate if the road network develops simultaneously with the appearance of new charcoal production areas.

3.3. WOOD VOLUME AND TREE LOSS ESTIMATION

The production of charcoal results in a loss of tree cover and biomass in the areas where this production occurs. The amount of charcoal produced within the study area, and the related wood burnt, can be estimated by linking the identified number and size of charcoal production sites with the production capacity of each site. To estimate the volume of timber used, I assumed the kiln mound to be comparable to a spherical cap. To calculate its volume, two values are needed: the height of the spherical cap (h), and the radius of the base circle (a).

$$V = \frac{\pi h}{6} (3a^2 + h^2) \quad \text{Spherical cap volume equation}$$

The average height of kilns has been reported to be 1.5 m (MPDES-CHE, 2004), but available pictures and videos show that this height is variable, and in certain cases it is clearly visible that it is higher than an adult man standing next to the kiln. Therefore, I assumed two possible kiln height values, 1.5 m and 2.0 m, with the latter being a conservative measure as it can be even higher. The radius of the kilns can be derived by the remote sensing data analysis, by measuring the dark circle of ashes left on the ground, once kilns are opened and charcoal is collected.



Figure 9 – Timber mound before being buried. Screen shot from a Puntland Development Research Center (PDRC) video.

The timber stacking inevitably leaves gaps between timber pieces (Figure 9). Therefore, a percentage of the volume derived from the spherical cap equation has to be deducted. I assumed a range between 20% and 40% of volume subtraction to account for space occupied by air and other materials used for the kiln construction (grass and shrub for kiln lightning).

I used Bird and Sheperd (1989) publication as a reference for wood parameters estimation, because it considered a neighbouring area (see Section 2.1), presenting similar characteristics to my study area. Their study identified four tree species groups as having wood suitable for conversion to charcoal: *Acacia bussei*,

Acacia senegal, *Acacia tortilis*, *Terminalia* species. The charcoal industry has traditionally relied on *A. bussei* for charcoal production, because of its high density and exceptional strength, but, as it became less abundant due to constant exploitation, other species have started to be felled (Bird and Sheperd, 1989). These include *A. senegal* and species of *Terminalia*, both of which produce charcoal of good quality. Additionally, even species not suitable for the production of good charcoal, like *Commiphora* species, were reported to have been utilized.

For the present research I assumed an average wood-to-charcoal conversion efficiency of 20%. The decision was made based on the consideration that the reference studies for Somalia, conducted in the 80's (Robinson, 1988; Bird and Sheperd, 1989), were already indicating a consistent decrease in availability of *A. bussei* in neighbouring areas, and that, consequently, less efficient species were also used. Robinson (1988) reported an average conversion efficiency from wood to charcoal of 40 percent (on oven-dry basis) for *A. bussei* based on field tests in the Bay region, but also indicated that this was as low as 20-25 percent when using a variety of other species. Bird and Sheperd (1989) confirmed these findings, suggesting that 40% should be considered as the highest efficiency in charcoal conversion, and that the average can be as low as 25%: as they wrote, "Charcoal cutting changed from being a selective operation to be a non-selective. As stocks diminished all sizes and types of tree were being felled In fact". Bird and Sheperd (1989) also report that the flattened barrels used for kiln-covering had become more expensive and difficult to find, and had been substituted with brittle breaking sheeting or with bushes to hold the earth away from the charcoal. Moreover, a study conducted in the north eastern part of Somalia (MDPE-SCH, 2004) also report a significant depletion of *A. bussei*, and FAO experts opinion (personal communication) put the efficiency of similar surface mounded kiln as low as 20%. A recent ICRAF (2014) publication reports the wood-to-charcoal conversion efficiency for earth-mounded kilns to be even as low as 8 to 20%. In addition, the development of the charcoal trading from a national to an international market level, as indicated by UN Security Council reports (2012; 2013), transformed the production in Somalia into a large scale operation. The massive increment of charcoal production is very likely to have caused a lowering of conversion efficiency.

To properly estimate wood volume, two additional tree species-specific parameters are needed:

- Density: the mass of wood per unit of volume;
- Moisture: water is present in wood in bound form in cell walls, and as free water both inside cells and between cell cavities.

The first parameter affecting transformation of timber into charcoal is the wood moisture content. A detailed analysis conducted by Bird and Sheperd (1989) indicates an average live stems moisture content of 52% for *A. senegal* and 42% for *A. bussei*. While for dead stems the values are 13.7% and 12.9% respectively. In Robinson (1988) analysis the moisture content range, for the *A. bussei* and *A. senegal* used in test sites, was recorded to be between 9 and 46 percent. Since visual analysis highlights a relation between charcoal production sites and systematic destruction of vegetation, it is very likely that not only dead stems are collected: any tree in the exploited areas is felled, mostly including green trees. The timber moisture for the wood volume calculation was consequently set to 47%, average between *A. senegal* and *A. bussei* live stems values (Bird and Sheperd, 1989).

A second parameter needed for calculating the kiln's charcoal production capacity is the timber density. Robinson (1988) measured an average oven-dry (0% moisture content) timber density of 928 kg/m³ for *A. bussei*, and 656 kg/m³ for *A. senegal*. The average timber density of *A. tortilis* is 690 kg/m³ (FAO 1991), while *Terminalia* spp (*Terminalia brownii*, *Terminalia prunioides*, *Terminalia spinosa*) ranges between 400 and 750 kg/m³ (KEFRI, 2005). Considering the indicated shortage of *A. bussei*, I assumed the dry-wood density as a range between 500 kg/m³ and 700 kg/m³.

Finally, the loss of tree cover was estimated by assuming the trees density to be 3,400 per square kilometre, measured in a previous study by visual interpretation of ten sites of one hectare on a 2006 Quickbird image (0.65 m) subset of the study area (Rembold et al., 2013). The same study suggested an average production of two bags of charcoal per single tree.

4. RESULTS

4.1. CHARCOAL SITE DETECTION

The rule set developed for the 1x1 km pilot area identified 68 sites in this area, out of the 75 sites visually counted. All sites identified by the object based image analysis were actual sites, while the seven undetected sites had irregular non-circular shapes or reflectance values above the threshold. Following the effective tuning of the rule set to accurately detect charcoal production sites for the training set, the method was extended to the entire study area.

Table 2 shows the accuracy assessment results for the randomly selected sample of 1x1 km clusters, separately for each image date. The performance of the rule set is different for each date, with highest user's and producer's accuracy obtained for the dataset of 3 March 2011, and the worst for 18 February 2011.

To investigate the origin of the different performances, the image metadata files were compared, and a visual assessment of the classification results was performed for each random cluster. For example, the visual assessment of a cluster containing no visually interpreted kiln sites, but many semi-automatically detected (Figure 10), revealed that the semi-automated procedure gave an entirely erroneous detection for both 2011 and 2013 scenes. Reflectance and roundness values of the wrongly classified objects are in the same range as those of charcoal sites correctly identified on other images from the same dates. The misdetection in this case is caused by the particular vegetation that has low reflectance and is sufficiently high to cast large shadows. Lack of field data makes it impossible to identify the vegetation type and therefore disclose the origin of the problem. Examination of Digital Elevation Models (SRTM and ASTER GDEM) did not reveal any particular variation in elevation within the cluster that might indicate higher water retention as compared to the surroundings.

A similar problem arose for areas that were burned by wildfires: the brightness values of burnt vegetation is equal to that of charcoal production sites. Moreover, in some cases burnt areas appear in patchy forms (likely areas where processes such as vegetation re-growth and wind depositing soil material are taking place), making it impossible for the rule set to discern them from charcoal sites based on their size.

Table 2 - Accuracy assessment results

Date	Total Visual	Total Semi-Auto	Visual \cap Semi-Auto	Producer's Accuracy	User's Accuracy
18-Feb-11	735	660	472	64.2%	71.5%
03-Mar-11	685	523	496	72.4%	94.8%
19-Feb-13	1512	1113	991	65.5%	89.0%
23-Feb-13	275	228	180	65.5%	78.9%

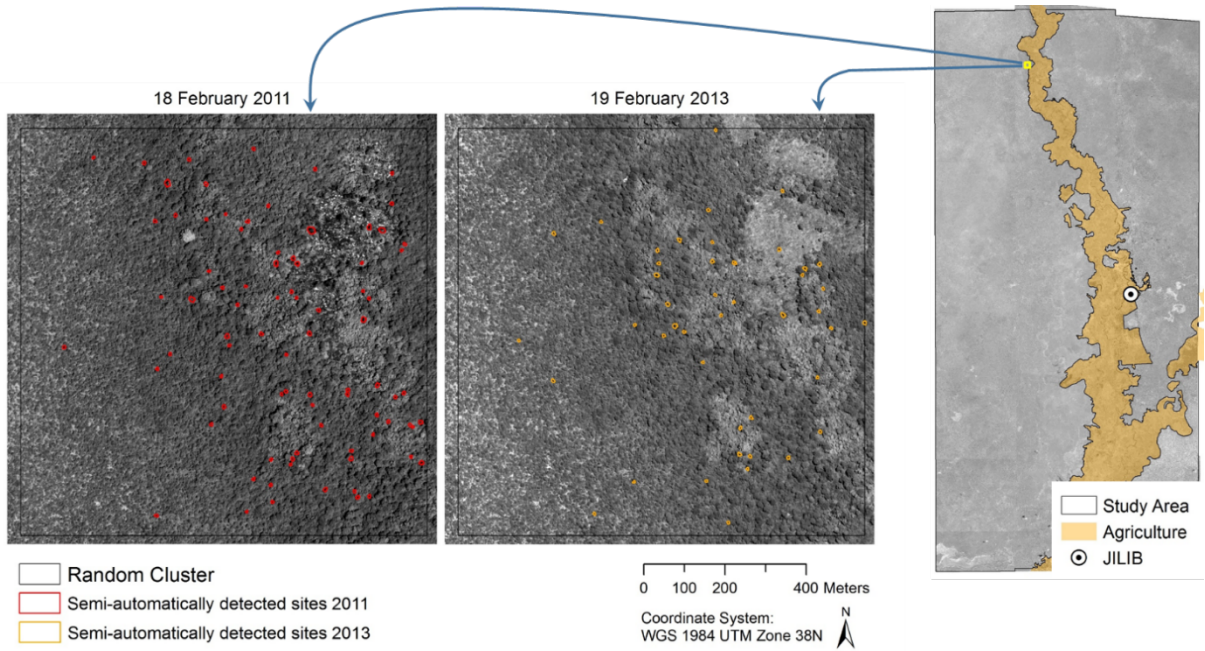


Figure 10 – Visual interpretation of a 1x1 km cluster with semi-automatically detected sites, but no visual counts. It reveals that erroneously detected sites are due to shadows, caused by a land cover type composed by dark and tall vegetation.

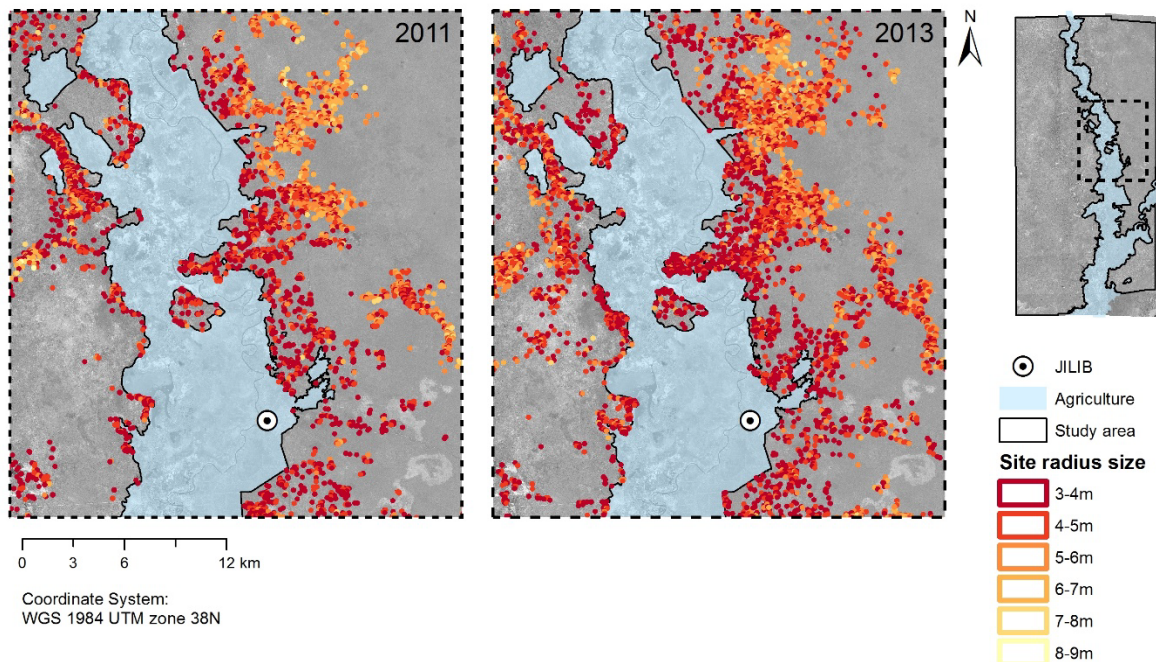


Figure 11 – Example of semi-automatically detected charcoal sites grouped by radius size.

The semi-automatically identified sites were grouped based on their size, with a one meter radius increase (ranging from a radius of 3 meters to 9 meters - Figure 11). Table 3 reports the user's accuracy of the semi-automated detection grouped by site size. From the results, it emerges that generally the lowest accuracy is obtained for the smaller sites (3 to 4 m radius), while it improves as the radius increases. This is due to the fact that small sites can be similar in size to tree shadows, while it is unlikely that trees cast shadows with sizes comparable to the larger sites. The poorer classification performance of images from 18 February 2011, and to a lesser extent 23 February 2013, can be explained by the higher presence of shadows casted by trees,

due to the particular elevation and azimuth angles of Sun and satellite at the time of image acquisition (see Table 1, Section 2.2). These larger shadows are detected by the semi-automatic analysis and counted as charcoal sites, resulting in a decrease of user's accuracy. In fact, not just shadows, but a combination of shadows, dark soil and dark vegetation, which present reflectance as low as the one of charcoal sites, can cause detection errors as, for example, the three wrongly classified sites in the classes 7-8 m and 8-9 m of 18 February 2011 (Table 3).

Another source of inaccuracy is the use of visual interpretation, in replacement of ground truthing, to perform the accuracy assessment. The visual interpreter account for charcoal sites without actually measuring roundness and size of each site. For example, a site could be interpreted as such and accounted for even though it is smaller than the threshold size set in the semi-automatic analysis (3 m radius). This leads to a number of sites counted by the photo interpreter, and used for the accuracy assessment, that are instead not accounted for by the rule set. The result is a low producer's accuracy that ranges between 64.2 and 72.4 percent, meaning that part of the charcoal sites visually counted were not detected semi-automatically. On the other hand, reducing the rule set size threshold would cause the detection by the semi-automatic procedure of smaller sites, but also of many smaller shadows, thus decreasing the producer's accuracy.

The intersection of the visually counted sites with the 200 m buffer created around the semi-automatically detected sites, reveals that many of the sites missed by the execution of the rule set, fall within the buffer (Table 4). A visual inspection of sites not falling within the buffer reveal that they are sites with a radius size smaller than 3 m, accounted for by the interpreter, but below the rule set threshold size. This indicates that the semi-automatic analysis provides indeed a good indication of dominant production areas, even without capturing the totality of the sites. It can be explained by the fact that charcoal is currently produced in a systematic way by concentrating efforts in areas where numerous trees are present and therefore many sites can be built.

Table 3 – Classification results by site size.

<i>18-Feb-11</i>				<i>03-Mar-11</i>			
<i>Site size (radius)</i>	<i>Visual counts</i>	<i>Semi-auto detected</i>	<i>User's accuracy</i>	<i>Site size (radius)</i>	<i>Visual Counts</i>	<i>Semi-auto detected</i>	<i>User's accuracy</i>
<i>3-4m</i>	260	400	65.00%	<i>3-4m</i>	171	187	91.44%
<i>4-5m</i>	141	173	81.50%	<i>4-5m</i>	131	137	95.62%
<i>5-6m</i>	46	56	82.14%	<i>5-6m</i>	95	98	96.94%
<i>6-7m</i>	20	23	86.96%	<i>6-7m</i>	80	83	96.39%
<i>7-8m</i>	3	5	60.00%	<i>7-8m</i>	13	14	92.86%
<i>8-9m</i>	2	3	66.67%	<i>8-9m</i>	4	4	100.00%
<i>Total</i>	472	660	71.52%	<i>Total</i>	494	523	94.46%

<i>19-Feb-13</i>				<i>23-Feb-13</i>			
<i>Site size (radius)</i>	<i>Visual counts</i>	<i>Semi-auto detected</i>	<i>User's accuracy</i>	<i>Site size (radius)</i>	<i>Visual counts</i>	<i>Semi-auto detected</i>	<i>User's accuracy</i>
<i>3-4m</i>	405	501	80.84%	<i>3-4m</i>	93	136	68.38%
<i>4-5m</i>	285	305	93.44%	<i>4-5m</i>	60	65	92.31%
<i>5-6m</i>	183	189	96.83%	<i>5-6m</i>	26	26	100.00%
<i>6-7m</i>	92	92	100.00%	<i>6-7m</i>	1	1	100.00%
<i>7-8m</i>	25	25	100.00%	<i>7-8m</i>			
<i>8-9m</i>	1	1	100.00%	<i>8-9m</i>			
<i>Total</i>	991	1113	89.04%	<i>Total</i>	180	228	78.95%

Table 4 – Producer's accuracy

18-Feb-11	Visual	Producer's accuracy	03-Mar-11	Visual	Producer's accuracy
<i>Visual ∩ Semi-auto</i>	472	64.2%		494	72.1%
<i>Visual within buffer</i>	676	92.0%		642	93.7%
<i>Total Visual</i>	735			685	
19-Feb-13			23-Feb-13		
<i>Visual ∩ Semi-auto</i>	991	65.5%		180	65.5%
<i>Visual within buffer</i>	1445	95.6%		250	90.9%
<i>Total Visual</i>	1512			275	

4.2. CHANGE DETECTION

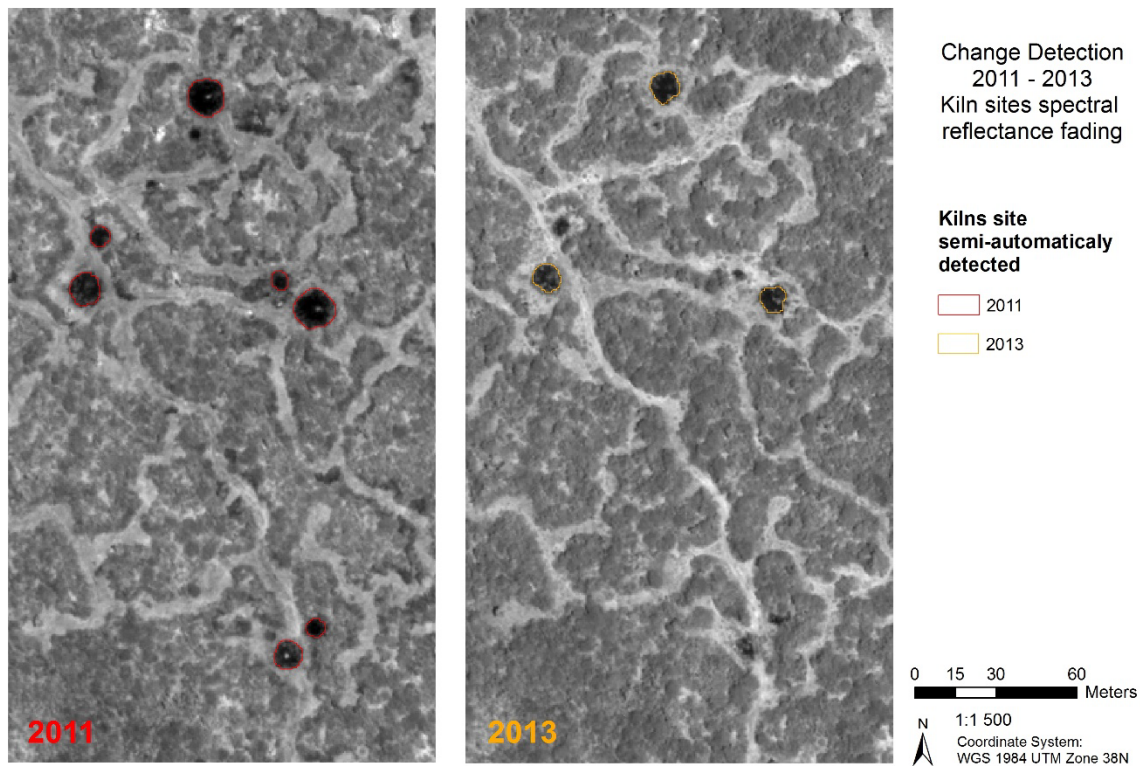


Figure 12 – Subset of the study area showing clearly visible charcoal production sites in 2011 (left) that are becoming less visible in 2013 (right), i.e. several years after charcoal is produced in the site.

Sites present on both dates have an average smaller size on the more recent date, which was expected as sites are used only once: gradually the spectral reflectance increases as winds cover the site with soil material, organic matter is decomposed in the soil, charcoal ash is washed away by rain, or new vegetation emerges on the site. Figure 12 shows an example of charcoal sites that appear larger and darker in 2011 compared to 2013. Sites observable on March 2011 imagery as very circular and evenly dark spots, are still visible on the February 2013 scenes, but have a higher reflectance and more irregular margins. Sites that remain detectable in 2013 have a radius of 4-5 m or larger. Smaller sites (3-4 m radius), which are visible on March 2011 images and were semi-automatically detected, on February 2013 imagery are instead barely visible and not detected by the rule set.

Within the sampled clusters, 483 charcoal production sites were visible on both 2011 and 2013 images. Out of these, 280 were semi-automated detected on 2013 scenes, equal to a producer's accuracy of 58.0%. Of the 1304 sites visible only on 2013 scenes, 891 were also detected semi-automatically, which translates into a 68.3% producer's accuracy. A higher producer's accuracy for more recent sites was expected as, compared to more recent sites, they display more regular round shape edges comprising evenly low reflectance values. Despite the clearly changing characteristics of the production sites, a simple rule to define age of sites by reflectance and roundness values could not be developed. These values variability largely depends on the initial segmentation settings, and on factors influencing the development of the site after charcoal production (i.e. wind and related soil transport, decomposition, rain-affected leaching of organic material, and vegetation regrowth). Generally speaking, we can say that kiln sites that appear as circular objects with homogeneously low reflectance are very likely to be recent. These sites are most probably less than 3 to 4 months old, since charcoal production is mostly carried out during dry season and images are from the Jilaal dry season (February/March), while the previous rain season (Dayr) ends in November.

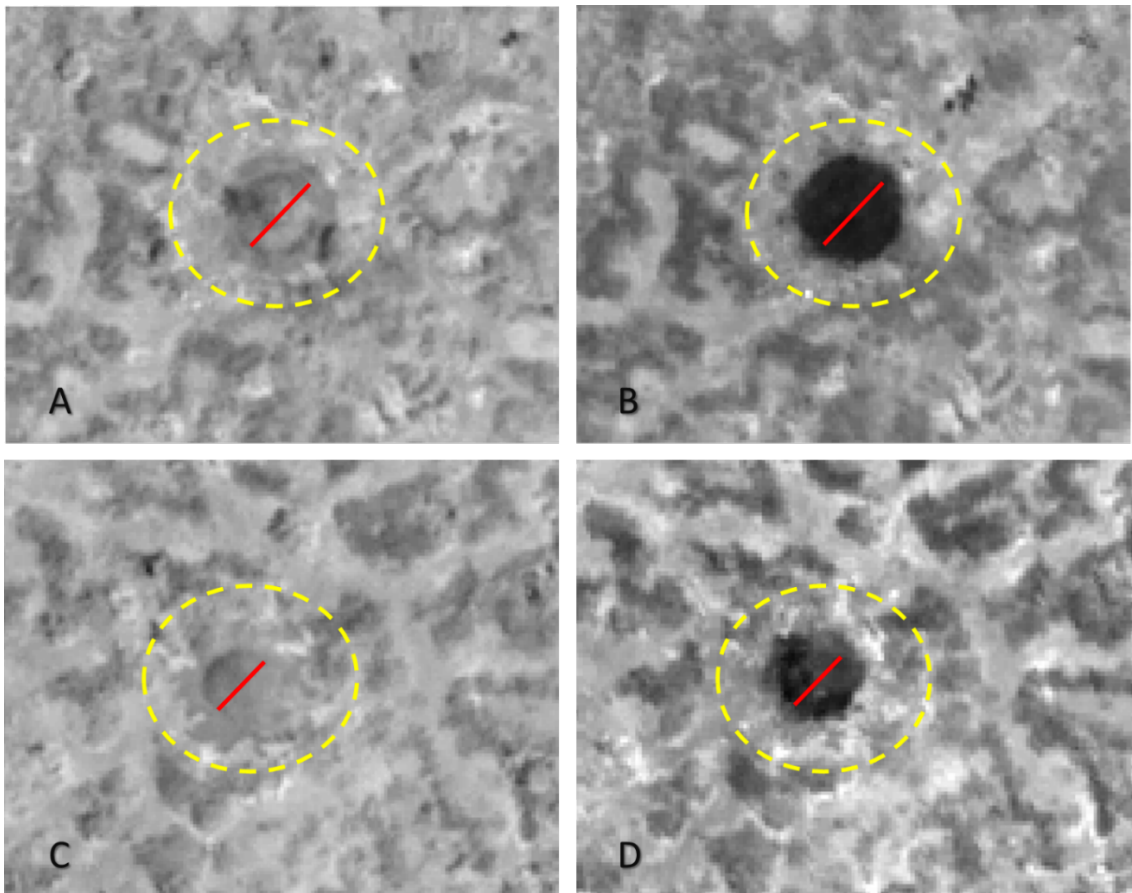


Figure 13 – Appearance of kiln covered by soil (A, C), and with remaining charcoal ashes exposed (B, D). A and C are from an 18 February 2011 scene, while B and D from 3 March 2011.

To better understand the relationship between kiln characteristics and the characteristics of the charcoal site originated from those kilns, I examined a few sites from a small area overlapping between 18 February 2011 and 3 March 2011. On these sites, kilns still covered by soil were present for the earlier date, while the charcoal was exposed on the more recent date (Figure 13). The site diameter changes slightly before and after exposure of the charcoal. An explanation is that charcoal ashes spread from workers while opening the site for faster cooling, leave on the ground a sign about one meter larger than the active kiln.

For the entire study area, 14,109 sites were detected on the 2011 scenes, of which 8,451 sites for the 18 February coverage, and 5,658 for 3 March. For 2013, 18,042 sites were detected, of which 15,009 on the 19 February, and 3,033 on the 23 February imagery. This translates in a 21.8% increase in the number of sites detected on 2013 scenes, compared to those detected on 2011 images. However, 3,267 sites were detected on both images, meaning that a number of sites can still be detected after two years. In fact, only 14,775 sites were detected solely on 2013 scenes, and hence built after March 2011 and before March 2013, giving a figure of 7,387 new sites every twelve months, within this period. Table 5 shows the number of site detected grouped by size, and accounts for the 1 meter reduction in sites radius size previously explained (Figure 13): numbers reported for 2013 consist of sites not previously detected on 2011 scenes. There is an overall increment of 4.5% in the number of sites, due mainly to an increase in site of medium-small radius, which means also an increase in charcoal production. The real increment between the two dates is higher as we should quantify the number of sites detected on 2011 images actually built in previous years. Unfortunately this cannot be done without images prior 2011.

Table 5 – Detected sites grouped by size. Number of sites detected on 2011 scenes, and number of sites for 2013 not previously detected on 2011 scenes. To be noted the overall increase in the number of sites.

	Sites detected on 2011	Sites detected on 2013 only	Difference
<i>2-3m</i>	7,518	7,838	+320
<i>3-4m</i>	3,743	3,835	+92
<i>4-5m</i>	1,694	1,948	+254
<i>5-6m</i>	875	906	+31
<i>6-7m</i>	233	227	-6
<i>7-8m</i>	42	19	-23
<i>Total</i>	14,105	14,773	+668

The accuracy of the developed semi-automatic method was determined for the sampled clusters, and by design should approximate the accuracy for all charcoal production sites detected in the study area. The image coverage of the study area is not equal between dates of the same year, hence an average accuracy was calculated by the sum of the visual counts for both dates of the same year, divided by the sum of the semi-automatically detected sites for both dates of the same year. This gives an overall user's accuracy of 81.7% for 2011 and 87.3% for 2013, while the producer's accuracy is 68.2% and 65.5% respectively. Despite the accuracy of the rule set being below 100%, the consistent approach used across all images allows for a reasonable interpretation of the changes in charcoal production sites between 2011 and 2013. Figure 14 shows the spatial distribution of charcoal sites in both years. The orange to dark red colours indicate areas with a large amount of sites per 1 km². Comparing the 2011 and 2013 results we can see that key production areas are located approximately in the same areas. However, 489 grids containing new charcoal production sites can be observed in 2013 across the study area. The changes are highlighted in Figure 15. The comparison of the sites distribution over the two year interval highlights the areas affected by recent charcoal production activities, thus providing a spatial overview of changes in key production zones (Figure 14 and Figure 15). The main high intensity production areas appear to remain the same, but 2013 shows an expansion of low intensity production sites.

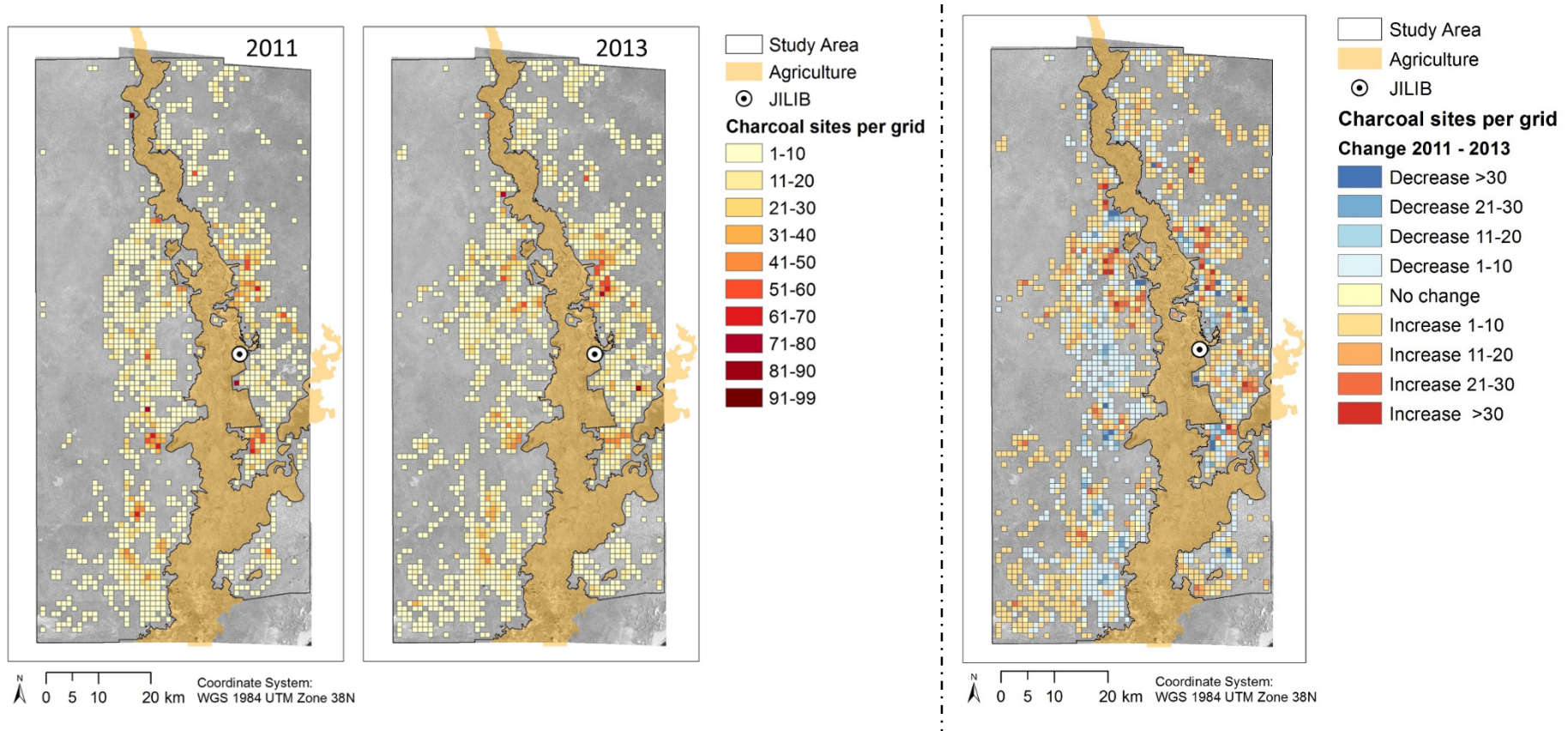


Figure 14 (left) – Spatial distribution of charcoal production detected with the object-based classification using 2011 and 2013 WorldView-1 imagery. Charcoal sites are grouped by 1x1 km grid cells, and coloured in yellow/red tonalities according to the number of sites per grid. Darker red correspond to grids containing a higher number of detected sites.

Figure 15 (right) – Map showing changes in the detected number of sites per grid (1x1 km) between 2011 and 2013.

A network comprising 2,468 km of dirt roads was digitized over the study area (Figure 16), of which 115 km were detected only on 2013 scenes. The new 2013 roads were all associated to new charcoal production sites, both in new production areas and in already active ones. In general, it was noted that routes running close to charcoal sites do not follow straight lines (Figure 17), but quite the opposite, indicating that the road network development seems to follow an opportunistic plan: to get as close as possible to the trees.

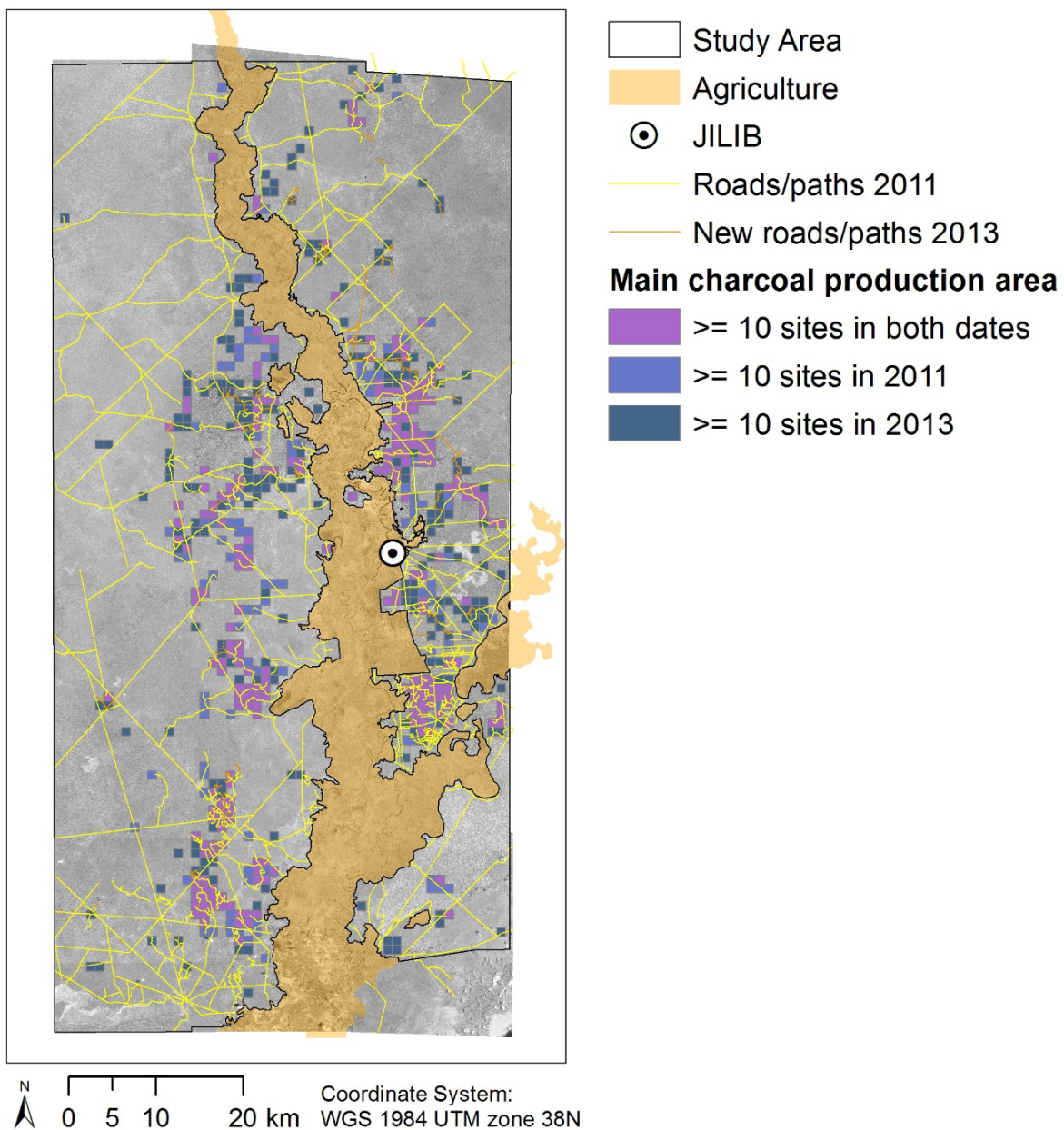


Figure 16 – Overview of main charcoal production areas that were semi-automatically detected, and visually-delineated road network. Straight lines are main dirt roads running through the bush land, while curved lines can be seen mostly in relation to charcoal production areas.

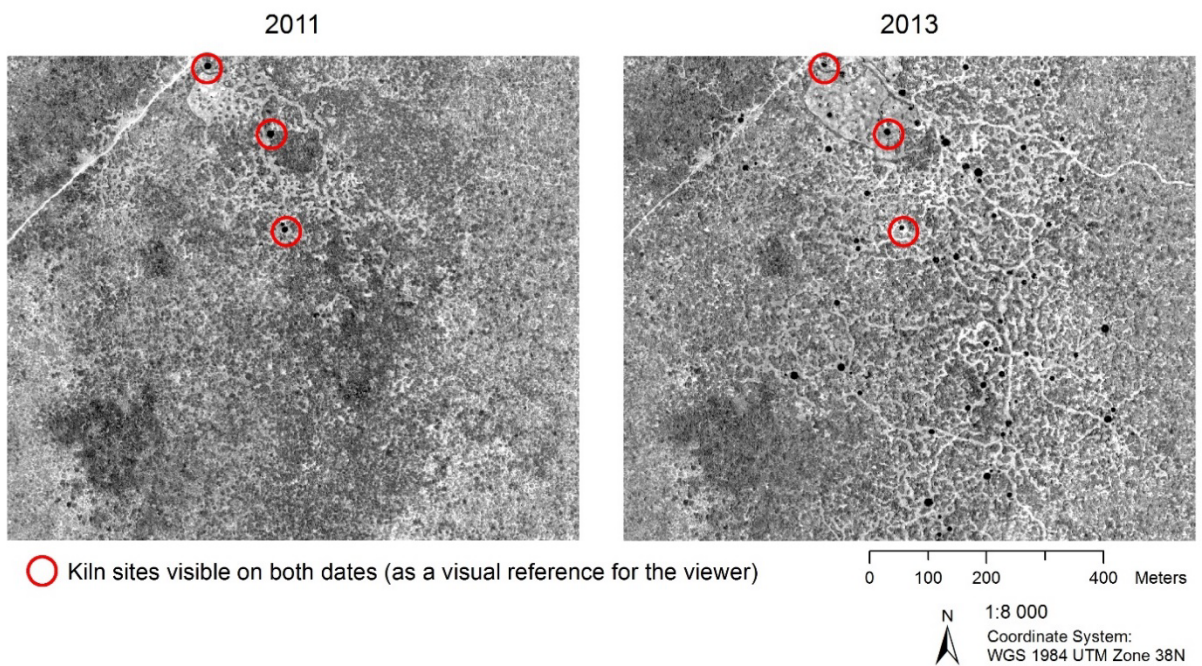


Figure 17 - Routes running close to charcoal sites do not follow straight lines. Example of the road network expansion between 2011 and 2013, with the purpose to access trees and produce charcoal. Note how new roads leads to new charcoal sites (black dots), following an opportunistic plan to get closer to trees.

4.3. WOOD VOLUME AND TREE LOSS ESTIMATION

Since precise information on vegetation composition and wood resources of the study area are not available, I derived values from studies conducted in other areas with similar vegetation (Robinson, 1988; Bird and Sheperd, 1989; refer to Section 3.3). The parameters are here presented as quantified ranges to leave the interpretation open to either conservative or more severe conclusions. Table 6 shows a summary of mean values and corresponding standard deviations of dry wood used, charcoal production, and charcoal bags produced, as calculated for each site radius. Complete tables, considering the respective minima and maxima of parameters values can be found in the Annex A (Tables A.1 and A.2). Regarding wood volumes, the lower estimate considers a kiln's height of 1.5 m, while 2.0 m gives the higher. For charcoal amounts, the mean and standard deviation are based on all possible combinations of the assumed low/high values of kiln height, volume air and other biomass (20 and 40%), and timber density (500 and 700 kg/m³). Following Rembold et al. (2013) assumptions, charcoal weights were translated to charcoal bags by dividing the weight by 27 kg.

Table 7 shows the estimates about the entire study area derived from semi-automatic detection, but considering sites identified uniquely on 2013 scenes, while excluding sites detected on both dates, as we cannot say when those sites were built. Also, all site radius size were reduced by 1 m to account for the potential actual kiln size versus semi-automatically measured (Section 4.2), thus providing more conservative estimates. A total 407,062.4 m³ mean of wood volume used was estimated, corresponding to 28,108.1 tons of charcoal produced and 1,041,039.0 bags.

Finally, the estimated tree loss rate for the study area, again only including sites uniquely detected on February 2013 scenes, is ranging between 1.2% and 5.3% (average 3.3%). The estimates were calculated considering the different assumed lower and upper values for kiln's height (1.5 - 2.0 m), content of air and other biomass (40% to 20%), and wood density (500 to 700 kg/m³), and assuming two charcoal bags produced per tree and a tree density of 3,400 per km² (Rembold et al., 2013). In terms of number of trees, it means that between 194,072 and 846,967 (average 520,520) trees were cut down after 3 March 2011, among the 15,980,000 trees potentially existing in 2006 (based on the tree density estimated by Rembold et al. (2013) - see Section 3.3).

Table 6 – From kiln size to quantification of dry wood used, and charcoal and charcoal bags produced. Reported values are averages. To determine the mean and standard deviation I used all combinations of assumed low/high values for dry wood used, charcoal production, and charcoal bags produced, calculated for each site radius.

Site Radius (m)	Dry Wood Mean (m ³)	Dry Wood Stddev (m ³)	Charcoal Mean (kg)	Charcoal Stddev (kg)	Bags Mean (No.)	Bags Stddev (No.)
2	5.3	2.5	675.2	451.6	25	17
3	10.5	4.6	1,328.8	846.0	49	31
4	17.8	7.5	2,243.7	1,398.2	83	52
5	27.2	11.2	3,420.1	2,108.2	127	78
6	38.6	15.7	4,857.8	2,975.9	180	110
7	52.2	21.1	6,557.0	4,001.4	243	148
8	67.8	27.2	8,517.6	5,184.6	315	192
9	85.5	34.2	10,739.6	6,525.6	398	242

Table 7 – Estimate of wood volume used and charcoal produced after March 2011. Values in the table refer to sites identified uniquely on 2013 scenes (not detected on 2011 scenes).

Site size	Number of sites	Wood vol. low ¹	Wood vol. high ²	Charcoal low ¹	Charcoal high ²	Bags low ¹	Bags high ²
m (radius range)	No.	m ³	m ³	tons	tons	No.	No.
2-3	7,838	52,633.4	203,556.8	2,789.6	15,103.9	103,317.4	559,404.2
3-4	3,835	52,860.6	167,065.7	2,801.6	12,396.3	103,763.5	459,121.3
4-5	1,948	46,128.2	128,924.3	2,444.8	9,566.2	90,547.9	354,303.0
5-6	906	32,981.3	85,009.0	1,748.0	6,307.7	64,741.1	233,617.3
6-7	227	11,793.6	28,715.8	625.1	2,130.7	23,150.4	78,915.4
7-8	19	1,336.3	3,119.8	70.8	231.5	2,623.1	8,573.7
Total	14,773	197,733.4	616,391.4	10,479.9	45,736.2	388,143.3	1,693,934.8

¹Low = 1.5 m kiln height, 40% air and other biomass, and 500 kg/m³ wood density.

²High = 2.0 m kiln height, 20% air and other biomass, and 700 kg/m³ wood density.

5. DISCUSSION

To detect charcoal production sites and the changes in their locations across a 4,700 km² area in southern Somalia from high-resolution panchromatic imagery, a rule set for object-based image analysis was developed in this study. Panchromatic scenes have the limitation of offering only one spectral band. Nonetheless, the developed rule set was able to provide satisfactory results in well discerning charcoal production sites on these images. Different sensor observation angles between image dates result in differences in shadow characteristics, which influence the interpretability of the images. Because larger shadows become similar in size and reflection to charcoal production sites, they negatively affected the detection process, impacting the analysis mostly in relation to smaller sites (3-4 m radius). In few cases, erroneous detection of larger production sites was recorded, and it was caused by the creation of erroneous segments due to a combination of shadows, dark soil, and dark vegetation. For the present study, the illumination conditions of acquired panchromatic WorldView-1 imagery were ideal for images of 3 March 2011 and 19 February 2013, allowing not incurring in such problems, while the conditions were more challenging for the other available dates (Figure 18). In most cases, when this confusion is present, it can be rapidly and effectively corrected-for through visual inspection of the results by an expert interpreter. However, for future image acquisition with the purpose of charcoal detection, the satellite's elevation and azimuth angles should be ideally similar to the Sun's elevation and azimuth to reduce confusion of production sites with shadows.

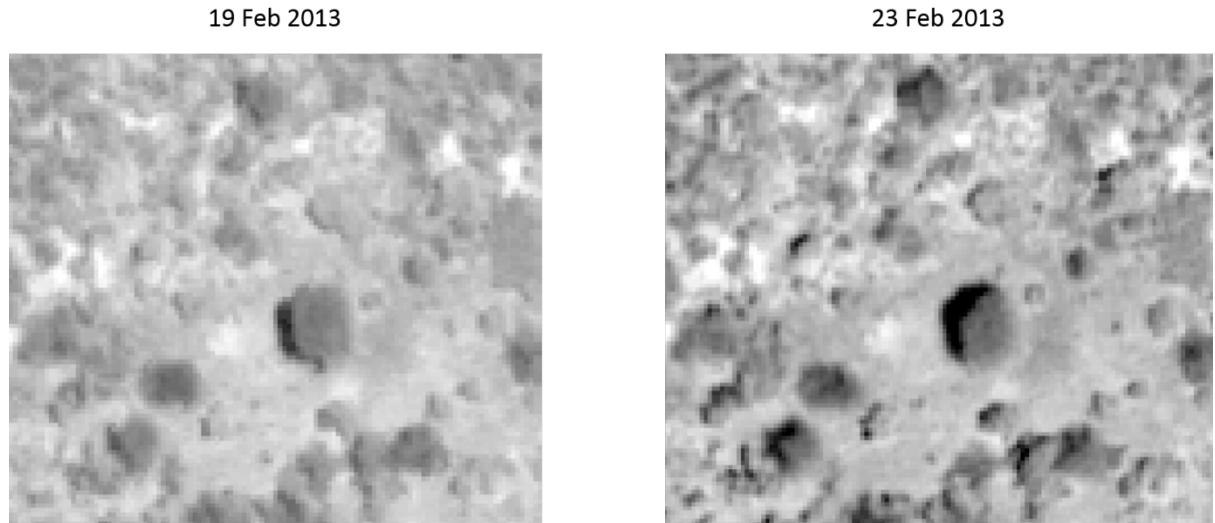


Figure 18 - Satellite record of the same area, showing shadow casting difference due to differences in elevation and sun angles of satellite and Sun. Angles are more similar in the image on the left (see Table 1), and looking at the tree in the middle, the recorded casted shadow is clearly smaller than the same tree on the right image.

Visual refinement of the semi-automated results of charcoal production site detection by an interpreter would be a much quicker and effective method as compared to the pure visual interpretation of the entire area. The refinement can be assisted in various ways:

- 1) As shown in this study, most actual sites occur within a buffer of 200 m around identified sites, hence an interpreter can focus largely on these areas;
- 2) More contextual information can be used, for example the presence of roads or locations of older sites. Regarding the first point, an improvement of the rule set could be attempted to include the detection of missed sites within the 200 m buffer previously discussed, and therefore produce better estimations. This would in turn involve longer time committed to a more complex rule set development, while the results

obtained with the presented methodology provide satisfactory results in an adequate amount of time. For the second point, roads and older sites location can be used as guidelines for a broader context analysis during visual interpretation in post-processing, which would help improving the results. For example, in areas away from roads and older sites, semi-automatically detected sites should be visually inspected as they have high chances to be incorrect (Figure 10). Moreover, signs of access roads, bare soil surrounding a dark object, or other sites nearby, are an indication for the interpreter that a specific dark spot missed by the semi-automatic detection, may be interpreted as a charcoal site.

Overall, the developed semi-automated procedure performed well, both objectively identifying the majority of total charcoal production sites and, through the use of a simple buffer, accurately locating the production areas. User's accuracy is high in most cases, proving that the risk of confusing charcoal production sites with other ground features with this method is low. One small disadvantage of the semi-automatic analysis, as compared to visual interpretation, is that the rule set is restricted to specific thresholds. With the semi-automatic procedure not all sites were detected, with mostly small sites being missed because of the difficulties in discerning them from shadows, dark vegetation and dark soil. On the other hand, while visual interpretation is more flexible, it is highly labour intensive, even when done by expert photo interpreters. In both cases, a higher frequency of image acquisition (ideally on a year basis, at the end of the main Jilaal dry season), is required to improve the identification of sites and changes in production locations and intensity. Concerning the spatial distribution of sites, it appears that smaller ones (3 to 4 m radius) are mainly concentrated within 5 km of agricultural areas (Figure 11), which are also the more accessible ones as most settlements are located here. This would suggest a charcoal production on a smaller scale, probably for domestic uses rather than for an industrial production directed to export. As supported by local expert knowledge, another explanation is that trees near agricultural areas were heavily logged in past years, not allowing for a sufficient coppice regeneration, and therefore leaving less timber for charcoal production. The detected charcoal production patterns seem to support that the recent large scale charcoal production, as the one promoted by Al Shabaab, concentrates first in areas where tree density is higher and distance from main roads, agriculture areas, and settlements is low, but also that as tree cover diminish, new access roads are built to exploit areas further away.

The analysis of very high resolution images through the semi-automatic method provided good estimates of charcoal sites size, which, as shown, can be used to derive estimates of wood volume used for charcoal production and amounts of charcoal produced. The values of the parameters necessary for calculating the estimates presented in this research (air/other biomass percentage per site, wood density and moisture, and kilns efficiency), were derived by studies conducted in other parts of Somalia. With the continued impossibility of conducting field data collection in southern Somalia, more accurate estimations could be only obtained by replicating the conditions found in the study area (i.e. building a series of kilns in the same way as in the study area, under the guidance of experts with local knowledge). Also, to quantify the charcoal production related tree cover loss, the estimations were done by using the same assumptions presented by Rembold et al. (2013) for a subset of the study area (density of 3,400 trees per km², and two charcoal bags produced per tree). These assumptions are quite simplistic as based on the analysis of a small area and on local experts' interviews, but aim mainly at providing a key range of tree loss in the area due to charcoal production. It is clear that any mistake in those assumptions would lead to a large mistake in the overall estimates. Nevertheless, the conservative figures provided by the present research highlight that the tree canopy is being lost at an alarming rate.

The loss of tree cover has a negative effect on the environment and consequently on people's life. For example, the loss of the protective tree layer has the direct consequence of increasing the underlying soil's vulnerability to erosion by exposing it to agents such as desiccating winds and heavy rains (FAO, 2007). A

complete list of the resilience effects provided by trees in the dry lands of Eastern Africa was presented in a recent publication by the World Agroforestry Center (ICRAF, 2014):

- Trees are less unstable than livestock and crops during drought, as their deep rooting system allows access to water resources (not available to other life forms);
- Trees experience little mortality during drought (unlike livestock) and normally recommence full production once drought is over;
- Trees provide goods and services (fodder and forage) during the period at the end of the dry season and the start of the rainy season, when foods from crops and livestock are insufficient to satisfy demand;
- Trees enhance soil fertility by recycling of nutrients from the deep soil horizons to the topsoil layers and by fixating atmospheric nitrogen;
- Trees provide erosion control by reducing water runoff and speed, and thus improving soil moisture and protecting land, making it available for settlement and agriculture;
- Trees sequester carbon and thus can generate income through the carbon emission trading system;
- Trees provide wood fuels.

Al-Shabaab is reported to be the main actor actively involved in the charcoal production business (UN Security Council, 2011) and therefore in the loss of tree cover. Extending the analysis to other parts of the country (depending on image availability) will result in a better overview of charcoal production zones, which could give indication of Al-Shabaab influence in the region. Nonetheless, also other armed groups may potentially profit from the incomes of large-scale charcoal production and consequently it may not be wise to focus the analysis of charcoal production solely on supposed Al-Shabaab territory.

A monitoring system of charcoal production in Somalia should be implemented starting from the methodology presented in this research, which gives a very detailed overview of a vast area of which previously very little was known. The primary limitations when monitoring large areas with very high spatial resolution include, not only the development of generic and robust methods to be able to replicate interpretation in a consistent way, but also the availability of required data sets, and having the resources to purchase such data (Hansen et al., 2008). Somalia is a large country ($637,657 \text{ km}^2$) and an updated land cover map would help highlighting areas with remaining high tree density, helping focusing the analysis on specific areas and therefore reducing the amount of expensive very high resolution images needed. The most recent wall-to-wall land cover map of Somalia was produced in 2002 from visual interpretation of Landsat TM (30m resolution, freely available) images, acquired mainly in the year 1999 (FAO, 2002). This could be updated at relative low cost and maintained up-to-date in the future using the upcoming Sentinel-2 satellite (10m resolution) or the already operational Landsat-8 (15m), both freely available. There is also interest in ‘up-scaling’ to assess the potential of lower resolution imagery in allowing effective detection of charcoal production sites, while reducing costs. The term ‘up-scaling’ refers to the use of information available at smaller scales to derive information at larger scales (Hay et al., 2001). Charcoal production sites identified with very high resolution imagery could be used as reference to relate fine scale with coarser scale. Furthermore, the coarser resolution imagery from Landsat-8 and Sentinel-2 hold multispectral information that should be investigated to evaluate whether they provide any advantage compared to panchromatic used in this research.

6. CONCLUSIONS

The results confirm the high level of suitability of Very High Resolution imagery for charcoal production monitoring in southern Somalia. They also make it clear that for larger areas, and consequently larger volumes of data, an automatic object detection approach can be a powerful and quite accurate way of monitoring charcoal production. The development of the semi-automatic approach and its execution, require less time and less human resources compared to a wall-to-wall visual interpretation. Visual interpretation is still needed as a ground truthing alternative, until the security situation will allow for an accurate field data collection. Field data collection would in turn contribute to reduce the level of subjectivity affecting the accuracy assessment of the present study, caused by visual interpreter skills and perception in identifying kiln sites. Additionally, a visual refinement of the semi-automated classification results would save a lot of time as compared to visual identification for the full area, while increasing the accuracy. The developed semi-automatic method succeeds not only in localizing main production area, but also in allowing for indicative quantification of charcoal produced. Even indicative estimates have their importance for most of the development activities, as they principally require good estimates of wood resources if environmental degradation is to be avoided. This research further contributes to the limited quantitative and spatial knowledge regarding charcoal driven deforestation in Southern Somalia by giving indications on the origin of the rapidly increasing amount of charcoal production and export. In fact, this research expands Rembold et al. (2013) study area to a hundred times larger area, and provides estimates about volume of timber used for charcoal production and related rate of tree cover loss. Despite the fact that the estimated 3.3% of tree loss refers to a very short period (2011-2013), it represents an alarming figure, in line with the 7.2% over 5 years (2006-2012) reported by Rembold et al. (2013). While further analysis to cover a broader period are recommended, the outcome of this research represents an important progress towards the establishment of a reliable charcoal production monitoring system.

LIST OF REFERENCES

- Akpalu, W., Dasmani, I., & Aglobitse, P. B. (2011). Demand for cooking fuels in a developing country: To what extent do taste and preferences matter? *Energy Policy*, 39(10), 6525-6531.
- Arnold, J. E. M., Köhlin, G., & Persson, R. (2006). Wood fuels, livelihoods, and policy interventions: Changing Perspectives. *World Development*, 34(3), 596-611.
- Baatz, M., Schaepe, A. (2000). Multiresolution segmentation – an optimization approach for high quality multiscale image segmentation. In: Strobl, J., T. Blaschke & T. Griessebener (Eds.) *Angewandte Geographische Information sverarbeitung* (AGIT-Symposium Salzburg), pp. 12-23.
- Bakonyi, J., & Abdullani, A. (2006). Somalia – No Central Government, But Still Functioning. *Agriculture & Rural Development*. GTZ International Services, 36-38.
- Bird, N.M., and Sheperd, G. (1989). Charcoal in Somalia: a wood fuel Inventory in the Bay Region of Somalia. Ministry of Livestock, forestry and range - Mogadishu, Somalia. National Range Agency.
- Boko, M., I. Niang, A. Nyong, C. Vogel, A. Githeko, M. Medany, . . . Yanda, P. (2007). Africa. Climate Change 2007: Impacts, Adaptation and Vulnerability. In O. F. C. M.L. Parry, J.P. Palutikof, P.J. van der Linden and C.E. Hanson (Ed.), *Contribution of Working Group II to the Fourth Assessment Report of the Intergovernmental Panel on Climate Change* (pp. 433-467). Cambridge, UK: Cambridge University Press.
- Clancy, J. S. (2008). Urban ecological footprints in Africa. *African Journal of Ecology*, 46(4), 463-470.
- Cooke, P., Köhlin, G., & Hyde, W. F. (2008). Fuelwood, forests and community management – evidence from household studies. *Environment and Development Economics*, 13(01), 103-135.
- DeFries, R., Achard, F., Brown, S., Herold, M., Murdiyarso, D., Schlamadinger, B., & de Souza Jr, C. (2007). Earth observations for estimating greenhouse gas emissions from deforestation in developing countries. *Environmental Science & Policy*, 10(4), 385-394.
- Drăguț, L., Tiede, D., & Levick, S. R. (2010). ESP: a tool to estimate scale parameter for multi-resolution image segmentation of remotely sensed data. *International Journal of Geographical Information Science*, 24(6), 859-871.
- Digital Globe (2010). Radiometric Use of WorldView-2 Imagery, Technical Note prepared by: Todd Updike, Chris Comp. (http://www.digitalglobe.com/downloads/Radiometric_Use_of_WorldView-2_Imagery.pdf)
- eCognition (2013). eCognition® Developer 8.9 - Reference Book. Trimble Germany GmbH.
- Espindola, G. M., Camara, G., Reis, I. A., Bins, L. S. and Monteiro, A. M. (2006). Parameter selection for region-growing image segmentation algorithms using spatial autocorrelation. *International Journal of Remote Sensing*, vol. 27, no. 14, pp. 3035–3040.
- FAO (1991). Energy for sustainable rural development projects - Case studies - Training materials for agricultural planning - 23/2. Food and Agriculture Organization of the United Nations, Rome.
- FAO (2002). Multipurpose Africover Database for Somalia – AFRICOVER. Food and Agriculture Organization of the United Nations, Rome.
- FAO (2005). Irrigation in Africa in figures. AQUASTAT Survey. FAO Water Reports 29. Food and Agriculture Organization of the United Nations, Rome.
- FAO (2007). Forests, trees and water in arid lands: a delicate balance. *Forests and water*. Unasylva No. 229. Vol. 58, 2007/4. Food and Agriculture Organization of the United Nations, Rome.
- FAO (2010). Criteria and indicators for sustainable wood fuels (Vol. 160). Food and Agriculture Organization of the United Nations, Rome.
- FAO (2013). FAO Statistical Database. Retrieved August, 2013, from <http://faostat.fao.org/>.

- FAO SWALIM (2010). Atlas of the Juba and Shabelle Rivers in Somalia. First Edition, March 2010. FAO Somalia Water and Land Information Management.
- FSNAU (2014). www.fsnaau.org/downloads/Lower-and-Middle-Juba-Agro-pastoral.pdf - Retrieved on 21/01/2014.
- Garoweonline (2014a). Somalia: Jubaland gains recognition after intense bilateral talks in Ethiopia. (http://www.garoweonline.com/artman2/publish/Somalia_27/Somalia_Jubaland_gains_recognition_after_intense_bilateral_talks_in_Ethiopia_printer.shtml) - Retrieved on 20/01/2014.
- Garoweonline (2014b). Somalia: Jubaland President Escapes Unhurt After Car Bomb Attack. (<http://allafrica.com/stories/201309130230.html>) - Retrieved on 20/01/2014.
- Ghilardi, A., Mwampamba, T., & Dutt, G. (2013). What role will charcoal play in the coming decades? Insights from up-to-date findings and reviews. *Energy for Sustainable Development*, 17(2), 73-74.
- Hay, G. J., Marceau, D. J., Dube, P., & Bouchard, A. (2001). A multi-scale framework for landscape analysis: Object-specific analysis and upscaling. *Landscape Ecology*, 16(6), 471-490.
- Hay, G. J., & Castilla, G. (2006). Object-based image analysis: strengths, weaknesses, opportunities and threats (SWOT). *ISPRS Archives*, Vol XXXVI/4-C42.
- Hansen, M. C., Roy, D. P., Lindquist, E., Adusei, B., Justice, C. O., & Altstatt, A. (2008). A method for integrating MODIS and Landsat data for systematic monitoring of forest cover and change in the Congo Basin. *Remote Sensing of Environment*, 112(5), 2495-2513.
- Holleman, C. F. (2003). The Socio-economic Implications of the Livestock Ban in Somaliland. Nairobi: Famine Early Warning Systems Network.
- ICRAF (2014). Jan de Leeuw, Mary Njenga, Bob Wagner and Miyuki Iiyama. Treesilience: An assessment of the resilience provided by trees in the dry lands of Eastern Africa. World Agroforestry Centre. Nairobi, Kenya. 166 pp.
- Kanninen, M., Murdiyarso, D., Seymour, F., Angelsen, A., Wunder, S., & German, L. (2007). Do trees grow on money?: The implications of deforestation research for policies to promote REDD. Bogor, Indonesia: Center for International Forestry Research (CIFOR).
- KEFRI (2005). Timber Information Bulletin No.3 - Classification of Wood Carving Species Using Macroscopic Properties. Kenya Forestry Research Institute - Forest Products Research Centre. Karura, Kenya.
- Kirkland E. mongabay.com, 23.01.2011. http://news.mongabay.com/2011/0123-somalia_kirkland.html, 2011.
- Köhrl, M., Magnussen, S. S., & Marchetti, M. (2006). Sampling methods, remote sensing and GIS multiresource forest inventory. Springer Verlag, Heidelberg, Germany, 403 p.
- McConnell T. Why charcoal may endanger Somalia's best hope for peace. Time world.27.11.2011; 2012. [<http://world.time.com/2012/11/27/why-charcoal-mayendanger-somalias-best-hope-for-peace/#ixzz2Sax0Rhep>].
- Miles, L., Newton, A. C., DeFries, R. S., Ravilious, C., May, I., Blyth, S., . . . Gordon, J. E. (2006). A global overview of the conservation status of tropical dry forests. *Journal of Biogeography*, 33(3), 491-505.
- MPDES-CHE (2004). Impact of Charcoal Production on Environment and the Socio Economy of Pastoral communities of Somaliland (pp. 37): Ministry of Pastoral Development & Environment, Somaliland & Candlelight for Health, Education & Environment.
- Oduori, S. M., Rembold, F., Abdulle, O. H., & Vargas, R. (2011). Assessment of charcoal driven deforestation rates in a fragile rangeland environment in North Eastern Somalia using very high resolution imagery. *Journal of Arid Environments*, 75(11), 1173-1181.

- Oduori, S. M., Vargas, R. R., Osman, A., & Rembold, F. (2009). Detection of Tree Cutting in the Rangelands of North Eastern Somalia Using Remote Sensing Technical Project Report L-15. Nairobi, Kenya: FAO-SWALIM.
- Omuto, C. T., Vargas, R. R., Alim, M. S., Ismail, A., Osman, A., & Iman, H. M. (2009). Land Degradation Assessment and a Monitoring Framework in Somalia Project Report L-14. Nairobi, Kenya: FAO-SWALIM.
- Oroda, A. S., Oduori, S. M., & Vargas, R. R. (2007). Applications of Remote Sensing Techniques for the Assessment of Pastoral Resources in Puntland, Somalia Project Report No. L-11. Nairobi, Kenya: FAO-SWALIM.
- Ryan, C. M., Hill, T., Woollen, E., Ghee, C., Mitchard, E., Cassells, G., . . . Williams, M. (2012). Quantifying small-scale deforestation and forest degradation in African woodlands using radar imagery. *Global Change Biology*, 18(1), 243-257.
- Rembold, F., Oduori, S. M., Gadain, H., & Toselli, P. (2013). Mapping charcoal driven forest degradation during the main period of Al Shabaab control in southern Somalia. *Energy for Sustainable Development*, 17(5), 510-514.
- Ribot, J. C. (1998). Theorizing Access: Forest Profits along Senegal's Charcoal Commodity Chain. *Development and Change*, 29(2), 307-341.
- Robinson, A.P. (1988). Charcoal-making in Somalia: a look at the Bay method. *Tropical forestry action plan for Latin America*. Unasylva - No. 159. Rome, Italy.
- Runge (1998). Runge, D.; Wesseler, J. and Waibel, H. 1998. The economic value of trees in agrosilvo-pastoralist systems of Sub-Saharan Africa. Paper presented at the World Congress of Environmental and Resource Economics, Venice, June 25-27, 1998
- Stumpf, A., & Kerle, N. (2011). Object-oriented mapping of landslides using Random Forests. *Remote Sensing of Environment*, 115(10), 2564-2577.
- UCS (2011). D. Boucher, P. Elias, K. Lininger, C. May-Tobin, S. Roquemore, and E. Saxon. The Root of the Problem: What is driving tropical deforestation today? - Tropical Forest and Climate Initiative. Union of Concerned Scientists. 126 pp.
- United Nations. Report of the Monitoring Group on Somalia and Eritrea pursuant to Security Council resolution 2002 (2011), (S/2011/433); 2011.
- United Nations. Report of the Monitoring Group on Somalia and Eritrea pursuant to Security Council resolution 2002 (2011), resolution 2036 (2012); 2012a.
- United Nations. Report of the Monitoring Group on Somalia and Eritrea pursuant to Security Council resolution 2002 (2011), (S/2012/544); 2012b.
- UN Security Council. (2011). Report of the Secretary-General on the protection of Somali natural resources and waters.
- UN Security Council. (2012). Resolution 2036 (2012) and Resolution 2060 (2012).
- UN Security Council. (2013). Report of the Monitoring Group on Somalia and Eritrea pursuant to Security Council resolution 2060 (2012): Somalia. In S/2013/413 (Ed.).
- UNEP. (2005). The State of the Environment in Somalia: A Desk Study: UNEP/Earthprint.
- Xiaoxia, S., Jixian, Z., Zhengjun L. (2005). A comparison of object-oriented and pixel-based classification approaches using Quickbird imagery. In 3rd International Symposium on Remote Sensing and Data Fusion Over Urban Areas (URBAN 2005), China, August 27-29.
- Wardle, P. & Pontecorvo, F. 1981. Special enquiry on fuel wood and charcoal. Paper presented to the UN Conference on New and Renewable Sources of Energy, Nairobi, Kenya, 10-21 August.
- White, F. (1983). The vegetation of Africa, a descriptive memoir to accompany the UNESCO/AETFAT/UNSO vegetation map of Africa. *Natural Resources Research* 20, 1-356.

- Whiteman, A., Broadhead, J., & Bahdon, J. (2002). The revision of wood fuel estimates in FAOSTAT. *Unasylva* 211, 53(4), 41-45.
- Woodcock, C. E., & Strahler, A. H. (1987). The factor of scale in remote-sensing. *Remote Sensing of Environment*, 21(3), 311-332.
- Zulu, L. C., & Richardson, R. B. (2013). Charcoal, livelihoods, and poverty reduction: Evidence from sub-Saharan Africa. *Energy for Sustainable Development*, 17(2), 127-137.

ANNEX A: CALCULATION OF WOOD VOLUMES AND CHARCOAL PRODUCTION

Table A.1 – From kiln size to volume of wood

Site radius size (m)	Site height (m)	Vol sphere cap (m ³)	Wood vol low (m ³)	Wood vol high (m ³)	Dry wood low (m ³)	Dry wood high (m ³)
			A	B	A	B
2	1.5	11.2	6.7	9.0	3.6	4.7
3	1.5	23.0	13.8	18.4	7.3	9.7
4	1.5	39.5	23.7	31.6	12.6	16.7
5	1.5	60.7	36.4	48.5	19.3	25.7
6	1.5	86.6	52.0	69.3	27.5	36.7
7	1.5	117.2	70.3	93.8	37.3	49.7
8	1.5	152.6	91.5	122.1	48.5	64.7
9	1.5	192.6	115.6	154.1	61.3	81.7
2	2	16.8	10.1	13.4	5.3	7.1
3	2	32.5	19.5	26.0	10.3	13.8
4	2	54.5	32.7	43.6	17.3	23.1
5	2	82.7	49.6	66.2	26.3	35.1
6	2	117.3	70.4	93.8	37.3	49.7
7	2	158.1	94.9	126.5	50.3	67.0
8	2	205.3	123.2	164.2	65.3	87.0
9	2	258.7	155.2	206.9	82.3	109.7

A : -40% air and other biomass

B : -20% air and other biomass

Table A.2 – From kiln size to amount of charcoal produced

Site radius size (m)	Site height (m)	Dry wood low (kg) (A)(C)	Dry wood high (kg) (B)(C)	Charcoal low (kg) (A)(C)	Charcoal high (kg) (B)(C)	Bags low No. (A)(C)	Bags high No. (B)(C)
2	1.5	1,779.5	2,372.7	355.9	474.5	13	18
3	1.5	3,652.7	4,870.3	730.5	974.1	27	36
4	1.5	6,275.1	8,366.8	1,255.0	1,673.4	46	62
5	1.5	9,646.8	12,862.5	1,929.4	2,572.5	71	95
6	1.5	13,767.8	18,357.1	2,753.6	3,671.4	102	136
7	1.5	18,638.1	24,850.8	3,727.6	4,970.2	138	184
8	1.5	24,257.6	32,343.5	4,851.5	6,468.7	180	240
9	1.5	30,626.4	40,835.2	6,125.3	8,167.0	227	302
2	2	2,664.1	3,552.1	532.8	710.4	20	26
3	2	5,161.6	6,882.2	1,032.3	1,376.4	38	51
4	2	8,658.2	11,544.3	1,731.6	2,308.9	64	86
5	2	13,153.8	17,538.5	2,630.8	3,507.7	97	130
6	2	18,648.5	24,864.7	3,729.7	4,972.9	138	184
7	2	25,142.2	33,522.9	5,028.4	6,704.6	186	248
8	2	32,634.9	43,513.2	6,527.0	8,702.6	242	322
9	2	41,126.6	54,835.5	8,225.3	10,967.1	305	406
Site radius size (m)	Site height (m)	Dry wood low (kg) (A)(D)	Dry wood high (kg) (B)(D)	Charcoal low (kg) (A)(D)	Charcoal high (kg) (B)(D)	Bags low No. (A)(D)	Bags high No. (B)(D)
2	1.5	2,491.3	3,321.8	498.3	664.4	18	25
3	1.5	5,113.8	6,818.4	1,022.8	1,363.7	38	51
4	1.5	8,785.2	11,713.6	1,757.0	2,342.7	65	87
5	1.5	13,505.6	18,007.5	2,701.1	3,601.5	100	133
6	1.5	19,275.0	25,700.0	3,855.0	5,140.0	143	190
7	1.5	26,093.3	34,791.1	5,218.7	6,958.2	193	258
8	1.5	33,960.7	45,280.9	6,792.1	9,056.2	252	335
9	1.5	42,877.0	57,169.3	8,575.4	11,433.9	318	423
2	2	3,729.7	4,972.9	745.9	994.6	28	37
3	2	7,226.3	9,635.1	1,445.3	1,927.0	54	71
4	2	12,121.5	16,162.0	2,424.3	3,232.4	90	120
5	2	18,415.4	24,553.9	3,683.1	4,910.8	136	182
6	2	26,107.9	34,810.5	5,221.6	6,962.1	193	258
7	2	35,199.0	46,932.0	7,039.8	9,386.4	261	348
8	2	45,688.8	60,918.4	9,137.8	12,183.7	338	451
9	2	57,577.2	76,769.6	11,515.4	15,353.9	426	569
A		: -40% air and other biomass		C	: density 500 kg/m ³	Bags	: 27 kg each
B		: -20% air and other biomass		D	: density 700 kg/m ³		

